COUPLED SOIL MOISTURE, SOIL TEMPERATURE, AND SNOW DYNAMICS IN COMPLEX TERRAIN OF A SEMI-ARID MOUNTAINOUS WATERSHED

A Thesis

Presented in Partial Fulfillment of the Requirements for the

Degree of Master of Science

with a

Major in Water Resources

in the

College of Graduate Studies

University of Idaho

by

Sage A. Bryden

November 2013

Major Professor: Timothy Link, Ph.D.

Authorization to Submit Thesis

This thesis of Sage Bryden, submitted for the degree of M.S. and titled "Coupled Soil Moisture, Soil Temperature, and Snow Dynamics in Complex Terrain of a Semi-Arid Mountainous Watershed," has been reviewed in final form. Permission, as indicated by the signatures and dates below, is now granted to submit final copies to the College of Graduate studies for approval.

Major Professor: _____ Date: _____
Dr. Timothy Link

Committee Members: _____ Date: _____
Dr. Mark Seyfried

_____ Date: _____
Dr. Robert Heinse

Department Administrator: _____ Date: _____
Dr. Jan Boll

Discipline's College Dean: _____ Date: _____
Dr. Kurt Pregitzer

Final Approval and Acceptance by the College of Graduate Studies:

_____ Date: _____
Dr. Jie Chen

Abstract

Hydrometeorological data from opposing aspects and steep hill slopes spanning the rain-snow transition zone are lacking, but are needed to understand how climate changes may be manifested in complex terrain. To gain a better understanding of how these variables are coupled, automated sensors were installed throughout a semi-arid mountainous watershed. Results indicated measurable differences in snow cover, soil temperature, and soil moisture dynamics between opposing north- and south-facing slopes (NFS and SFS). Most notably, soil temperature differences at the same elevation on opposing hill slopes were similar in magnitude to soil temperature differences measured nearby at locations separated by 900 meters elevation. Soil water content trends revealed that the SFS reached maximum soil moisture deficit approximately one month earlier than NFS and the upper watershed region. A comparison of the results from this study was made with a conceptual model of hydrologic seasonality from a smaller semi-arid watershed and incorporated with a literature review of the effects of climate change on sagebrush ecosystems.

Acknowledgements

I would formally like to thank those who have made this body of work possible. Thank you to my adviser, Dr. Timothy Link, for guiding me through the research and writing process and introducing me to a wealth of resources and ideas. Many thanks to Dr. Mark Seyfried for even more ideas, unparalleled field and technical experience, and complete generosity both personally and professionally. To Dr. Robert Heinse, for committing time to this project, opening up his lab for my use, and assisting with the technicalities of testing soil properties. I would like to thank Pat Kormos for installing meteorological stations in Johnston Draw and several of the folks at the Northwest Watershed Research Center (NWRC) for their support and expertise including Mark Murdock, Barry Caldwell, and Adam Winstral. I could not have collected this data without you. I would also like to acknowledge the following grants from the National Science Foundation for funding this research: NSF CBET-0854553 and NSF EPS-0814387.

On a more personal note, I would like to extend many thanks to Andrew Bryden for supporting me in achieving my dreams. I owe you everything and cannot possibly account for all you've done to help make this happen. Thank you to my fellow students, Meghan Carter, Zion Klos, and Ryan Niemeyer, for your friendship, support, and sound advice. I would like to extend my gratitude to my field assistant, Magruder, for always being there when needed, and to Jim Kutzman and Mayrene Shawver for diligently steering me back on track. Many more friends and family remain unnamed, but you know who you are and your encouragements have meant much to me in this process. Thank you.

Table of Contents

List of Figures

List of Tables

Chapter 1. Introduction

Understanding the variability of snow cover, soil moisture, and soil temperature is paramount to further developing our knowledge of hydrologic dynamics in complex mountainous terrain. Topography influences hydrologic response at the watershed scale in a variety of ways. Variations in slope aspect and angle influence solar radiation inputs at the surface, affecting soil temperature, snowmelt rates, and evapotranspiration. Complex terrain is a factor in the spatiotemporal variations of soil moisture and ultimately, runoff generation processes and streamflow. Within these mountainous regions, snow melt, soil moisture, and soil temperature couple on seasonal and individual event time scales, and hydrologic response is dependent both on antecedent as well as event hydrometeorological conditions. Chauvin et al. (2011) noted that the interaction of complex terrain and heterogeneous vegetation result in highly variable snowmelt inputs over space and time. Variability in snow cover and snowmelt influences timing and delivery of water to the soil and potentially available soil water during the growing season (Bales et al., 2011), as well as late-season flows that depend on the storage and release of soil water (Reba et al., 2011). This, in turn, influences the heterogeneity of vegetative cover which likewise affect snowpack and evapotranspiration processes. The rate and timing of water inputs to soil, coupled with organic matter from vegetation, influence soil development and depth of the soil profile. These soil characteristics have a direct influence on water storage capacity as well as runoff generation. Quantification of coupled snow, soil moisture, and soil temperature dynamics in complex terrain are especially needed in the rain-snow transition zone to understand how climate change will be manifested in these regions.

As hydrologists search for improved methods of understanding the spatiotemporal variations of hydrologic fluxes and coupling of snow and soil dynamics in complex terrain, the need for hydrometeorological data representing complex topography increases. The majority of data in the hydrologic record are sourced from relatively flat areas, uninfluenced by factors such as hill slope and aspect. In mountainous regions, monitoring of hydrologic fluxes is lacking (Bales et al., 2006; Williams et al., 2009) and has been primarily been limited to measurements of snow water equivalent and streamflow (Bales et al., 2006). Continuous snow monitoring stations throughout the country are preferentially located at high elevations where winter snow cover is likely and

hence mid-elevation regions along the rain-snow transition zone are poorly represented. Additionally, these stations are often located at relatively level sites below the upper timberline. Other data needed for modeling hydrologic response in mountain catchments include spatial variability of soil moisture, discharge from lower order tributary streams, and ecological processes (Bales et al., 2006). There is also a need for monitoring infrastructure at the watershed scale to support regional hydrologic modeling. Point measurements of snow depth, snow density, soil moisture and precipitation are reasonably accurate, but the ability to extend these points to a spatially complex landscape is inadequate (Bales et al., 2006; Lyon et al., 2008). Advances in remote sensing have improved our ability to monitor large scale areas, yet data are insufficient for watershed scale resolution of variability in snowpack, soil moisture, and soil temperature. More detailed characterization of the interactions between complex terrain, precipitation phase, snowmelt, soil temperature, soil moisture, and vegetation is critical to the development of hydrologic models in cold regions (Williams et al., 2009) and predicting how semi-arid rangeland hydrology will respond to climate variability (Chauvin et al., 2011).

A large body of work researching the interaction of snow dynamics, vegetation, soils, and complex terrain in a semi-arid region has been conducted in the Valles Caldera of northern New Mexico. The small watersheds in the caldera are characterized by rhyolitic parent material, seasonal snow cover, a distinct monsoon season, mixed-conifer forest, and cover a wide range of elevations and aspects. Lyon et al. (2008) used a network of temperature/light sensors to monitor snowmelt and streamflow and observed snowmelt to occur earlier on southern and western aspects. A later study by Broxton et al. (2009) found isotopic variability and transit times (i.e. time between water entering and exiting the system) to be related to aspect. Mean transit time increased on more northerly facing slopes, most likely due to greater soil depth and more developed soil characteristics. In contrast, greater isotopic variability and shorter transit times were observed on south facing slopes. Beyond the research in the Valles Caldera, the majority of studies investigating interactions of complex terrain with hydrological processes have concentrated primarily on runoff generating mechanisms and how they relate to soil moisture conditions. In a semi-arid ponderosa pine forest in New Mexico, hill slope runoff processes were shown to depend on antecedent soil moisture conditions and include subsurface lateral flow, rapid macropore throughflow, and overland flow generated by infiltration-excess or frozen soils (Wilcox et al., 1997; Newman et al., 2004; Newman et al., 1998). Chauvin et al. (2011) examined a semi-arid rangeland catchment in southwestern Idaho and suggested that the soil moisture and groundwater deficit

must first be replenished before streamflow occurs. Following snowmelt in the catchment, there was a decoupling of root zone soil water from deep groundwater and additional precipitation only served to offset evapotranspiration and did not contribute to streamflow. For most studies focused on semi-arid mountainous watersheds a common theme emerges where lateral subsurface flow dominates runoff processes and the soil profile must be wetted at depth for intermittent streamflow to commence. The spatial variation of these regions, coupled with highly variable snow cover, influences soil moisture heterogeneity within the watershed. Therefore, understanding the link between snow cover and soil moisture is important for hydrologic predictions at the catchment scale (Bales et al., 2011).

This study builds on previous work identifying relationships between snow melt, soil moisture, and streamflow in semi-arid mountainous watersheds proximal to our study site. Grant et al. (2004) examined soil moisture storage in Reynolds Mountain East, a 0.36 km^2 snow-dominated watershed, encompassing a range of elevations (2020 to 2140 m) and vegetative cover. Despite high spatial variation in the amount of stored soil water, significant temporal stability between individual sites was observed. Soil moisture storage fell into 4 distinct categories: (1) no change in soil storage, (2) nearly uniform change in soil water pattern over the catchment caused by uniform water inputs, (3) nonuniform change in soil water pattern over the catchment in the absence of water inputs or outputs, and (4) nonuniform change in soil water pattern caused by nonuniform inputs or outputs. The first condition occurred during late summer and early fall when precipitation inputs were minimal and plant uptake had ceased, during periods of snow cover when water input was buffered, or during late winter and early spring when soils were near field capacity and additional water input was translated to stream flow. The second condition typically described fall and winter events (precipitation and melt) when water inputs increased soil water storage. While the third condition described nonuniform decreases in soil storage across the catchment during summer dry down. Condition four was attributed to discrete events, typically rain-on-snow causing unevenly distributed water fluxes, and was not frequently observed in the data. Streamflow response in the catchment was observed to correlate with snow melt events when soils were at field capacity and additional water inputs were transmitted quickly to streamflow. Water inputs from rain was typically stored in the soil column and not correlated with increases in streamflow. The study by Grant et al. describes spatiotemporal variability of soil moisture in a snow dominated catchment, but does not cover the rain-snow transition zone where soil moisture dynamics and streamflow generation events may be more complex. The closest analog to our

study site is by McNamara et al. (2005) where five distinct hydrologic seasons are put forth based on soil moisture and evapotranspiration.

In the study by McNamara et al. (2005), field measurements and computer simulations were used to develop a conceptual model of hydrologic seasonality and streamflow generation in Dry Creek, a small semi-arid ephemeral catchment in southwestern Idaho. The study was conducted in an east-west oriented catchment of 0.02-km^2, averaging 1620 m mean elevation, and was based on field data that transected a single hill slope spanning approximately 15 meters elevation. The five soil moisture conditions, or hydrologic seasons, identified were (1) a summer dry period, (2) a transitional fall wetting period, (3) a winter wet, low-flux period, (4) a spring wet, high-flux period, and (5) a late-spring drying period. During the summer dry period soil moisture content was low, evapotranspiration exceeded precipitation, and most precipitation was lost to evapotranspiration before the wetting front reached 15 cm depth. There was no subsurface lateral flow and the streambed was dry. The transitional fall wetting period was marked by fall precipitation that exceeded evapotranspiration demands. Moisture accumulated in the soil and the wetting front traveled deeper into the profile. The authors noted that once precipitation transitioned to snow, water input would decrease, leaving deeper soil zones relatively dry if the wetting front had not reached depth prior to snowfall. During the winter wet, low-flux period, soil moisture levels were near field capacity and relatively stable. Precipitation greatly exceeded evapotranspiration and occurred primarily as snow. Any water input to the soil depended on the energy balance of the snowpack. McNamara et al. (2005) demonstrated that the upslope and downslope regions of the catchment were hydraulically independent of each other during this period and that the beginning of the winter wet, low-flux season was associated with initiation of stream flow that continued through the winter. The shift to a spring wet, high-flux period occurred with the onset of seasonal snowmelt. During this period, precipitation greatly exceeded evapotranspiration and water inputs produced immediate streamflow responses. Lateral subsurface flow was completely connected along the hill slope, indicated by rapid soil moisture response at depth to water input. In the final phase, the transitional late-spring drying period was when water content in the soil declined from near field capacity to relatively dry. The rate of evapotranspiration was much higher than the rate of precipitation input and streamflow waned until finally going dry. From these five identified hydrologic seasons, a conceptual model was put forth describing streamflow generation in Dry Creek as dependent on evapotranspiration rates in relation to precipitation and hill slope connectivity of lateral subsurface flow. This is the best work

to date on hydrologic seasonality in semi-arid terrain, but it is spatially constrained. Hence, similar studies are needed from larger, more complex watersheds that span the rain-snow transition zone to understand how aspect and elevation affect hydrologic seasonality. We seek to expand on the conceptual model put forth by McNamara et al. (2005) and find out whether a proximal but more complex watershed functions similarly to the single hill slope discussed, or whether the conceptual model manifested differently across different components of the landscape (e.g. upper elevations, northern exposures, southern exposures)?

Our general objective is to improve understanding of the spatiotemporal variability and coupling of snow cover, soil moisture, and soil temperature and further develop our knowledge of hydrologic systems in complex mountainous terrain. Specific objectives are to: 1) Characterize the hydrometeorology of the landscape by examining variation in snow cover, soil temperature, and soil moisture at different elevations and slope aspects over annual cycles; 2) Examine streamflow generation by individual runoff producing events and along seasonal time-scales; 3) Test whether the general conceptual model proposed by McNamara et al. (2005) holds in a larger more complex watershed, or propose an alternative conceptual model for specific physiographic regions; and 4) Incorporate insights from this investigation with a literature review of the expected effects of climate warming on sagebrush ecosystems and implications for future resource management. Anticipated outcomes from this study are a detailed dataset of hydrometeorological variables that can be applied to better understanding of runoff processes and ecohydrology in complex terrain. The anticipated outcome of the research will be to improve hydrological and ecological models as well as facilitate understanding of climate change effects on mid-elevation regions in the rain-snow transition zone.

Chapter 2. Methods

2.1 Site Description

The study site is located in Johnston Draw, a 1.8 km^2 subbasin of the Reynolds Creek Experimental Watershed (RCEW) in southwestern Idaho (Figure 2-1). The catchment ranges in elevation from 1490-1850 meters, spanning the rain/snow transition zone with rain dominating the lower portion of the catchment and snow dominating the upper elevations. Johnston Draw is generally oriented east-west with steep north-facing and south-facing slopes in the lower portion of the watershed (19° average slope). The upper half of the watershed is characterized by lower relief terrain (9° average slope), and is dominated in the winter by large snow drifts. An ephemeral stream drains the catchment, typically yielding surface water from late fall to mid-summer (November through July).

Johnston Draw geology consists primarily of granitic rock with some quartz monzonite (Figure 2-2). Notable exceptions are the presence of olivine basalt at the mouth of the watershed (1490-1530 meters) and felsic basalt in the upper western portion of the watershed above 1770 meters. Opposing north and south-facing slopes are underlain by the same granitic rock. Despite consistent parent material, soil characteristics differ between opposing aspects. North-facing slopes tend to have deeper soils (70-150 cm) and finer texture compared to south-facing slopes with shallower soils (20-50 cm) and greater rock content. Soils on the North-facing slopes consist of coarse sandy loam, classified in the Ola series. South-facing slopes host a rocky coarse sandy loam in the Takeuchi series (Figure 2-2).

The climate is seasonal with cool moist winters and warm dry summers. Meteorological data spanning from the bottom of the catchment to the top indicate an average annual temperature of 7.4°C and 550 mm (21.5 in) average annual precipitation. The majority of precipitation occurs during the cold season as snow. There are mixed rain/snow and rain-on-snow events during late autumn, mid-winter, and early spring. Intermittent streamflow ranges from a dry channel during summer and early fall months (July to November) to 0.06-0.08 cms (2-3 cfs)

during peak runoff. Peak runoff typically occurs during early spring in March with additional high runoff events in April and May.

Johnston Draw vegetation is dominated by big sagebrush (*Artemesia tridentata* spp.) (Figure 2-2). Wyoming big sagebrush (*A. tridentata* spp. *wyomingensis*) mixed with bitterbrush and occasional juniper constitutes 25-50% of the vegetation cover on south-facing slopes. North-facing slopes are dominated by mountain big sagebrush (*A. tridentata* ssp. *vaseyana*) mixed with snowberry providing 50-75% vegetative cover. Quaking aspen is found in riparian areas and in isolated patches on the north-facing slopes. Above 1750 meters, in the upper half of the watershed, low sagebrush (*Artemisia arbuscula* Nutt.) and mountain big sagebrush can be found mixed with Idaho fescue and wheatgrasses.

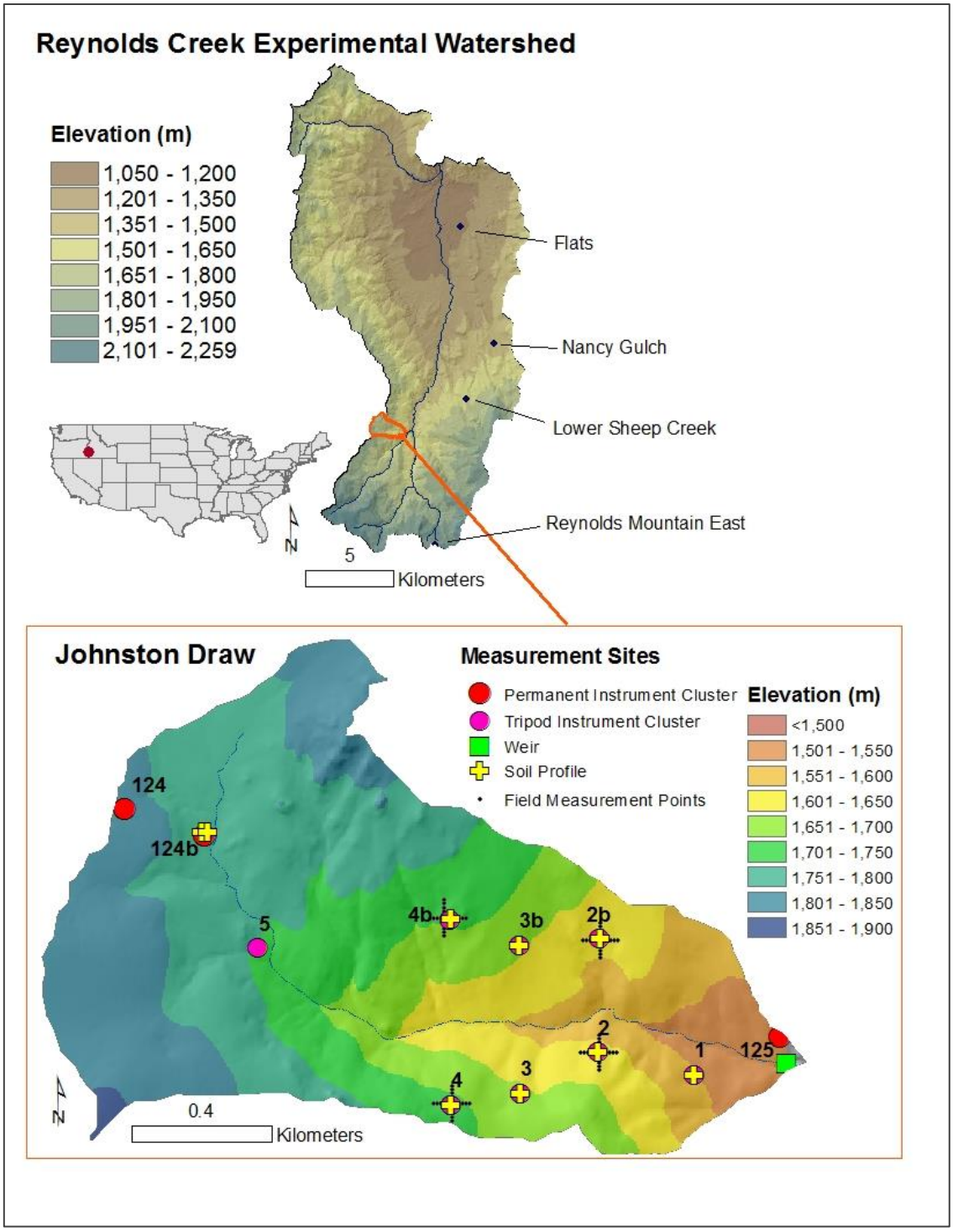

Figure 2-1. Location of field measurements in Johnston Draw, a subbasin of Reynolds Creek Experimental Watershed in southwestern Idaho.

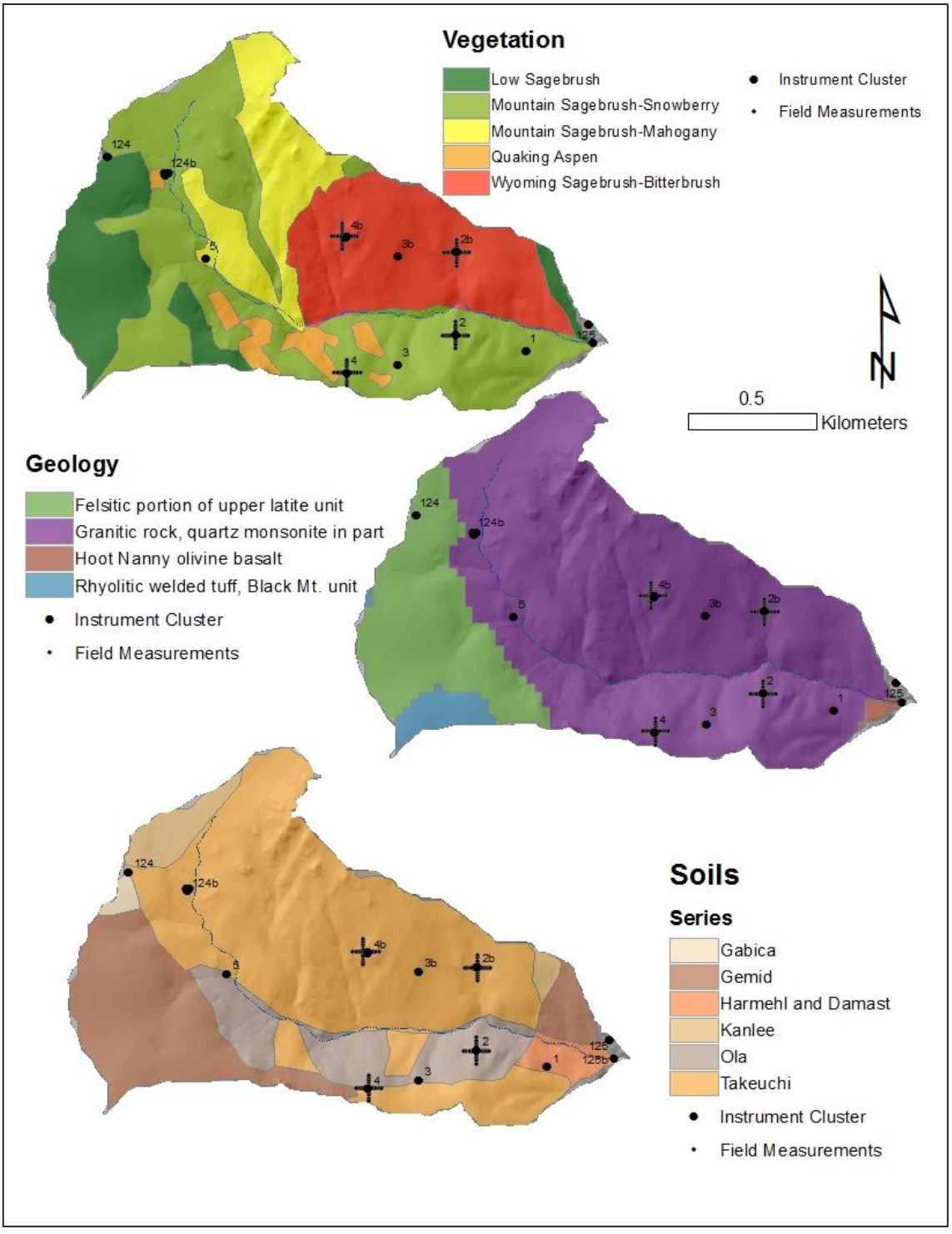

Figure 2-2. Vegetation, geology, and soils characteristics of Johnston Draw modified from the RCEW GIS layers (ftp://ftp.nwrc.ars.usda.gov/)

2.1.1 North-South Facing Slope Characteristics

The lower portion of Johnston Draw outlined in Figure 2-3 illustrates the slopes surrounding data collection efforts for this project. Six stations were located at paired elevations on opposing slopes: stations 2 and 2b at 1600 meters, stations 3 and 3b at 1650 meters, and stations 4 and 4b at 1700 meters. Based on a LiDAR-derived 5 meter digital elevation model (DEM), slopes surrounding the automated sites (Figure 2-3) range from 0-45° with an average of 19°. In this portion of the watershed south-facing slopes (SFS) average 17° gradient and north-facing slopes (NFS) average 22°. North-facing slopes tend to be slightly steeper than south-facing slopes with 61% of the north-facing area in the range of 20-30° and 70% of the south-facing area ranging between 10-20° (Figure 2-4).

Aspect also varies throughout the generally north- and south-facing slope areas where small crenulations in the topography create localized areas facing east and west. Both slopes have a large proportion of area facing eastward. The northern exposure consists of 71% of the surface area oriented between 315° and 45° (NNW, N, NNE) and 25% of the surface area oriented between 45° and 90° (ENE). The southern exposure has 57% of the surface area oriented between 135° and 225° (SSE, S, SSW) and 40% of the area oriented between 90° and 135° (ESE). Figure 2-4 illustrates orientation of topography at 5m scale.

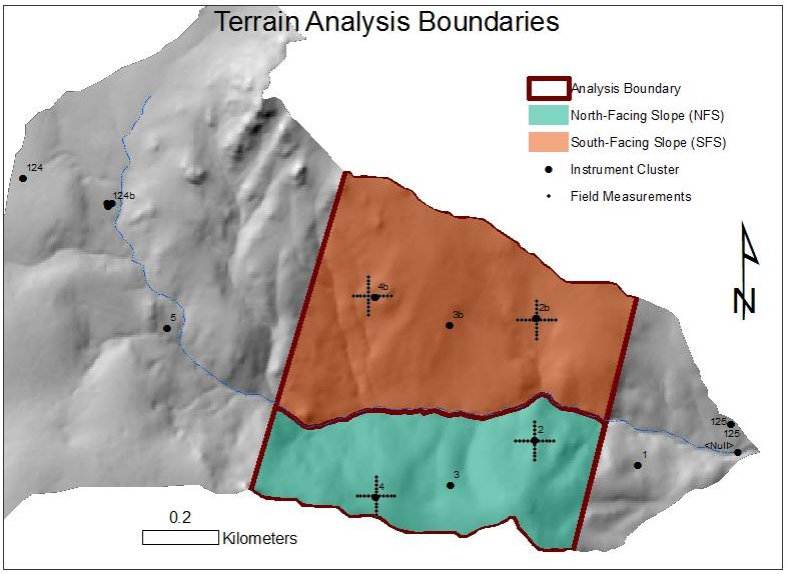

Figure 2-3. Analysis area used to determine terrain characteristics (e.g. aspect, slope, radiation angle) of north- and south-facing slopes in Johnston Draw.

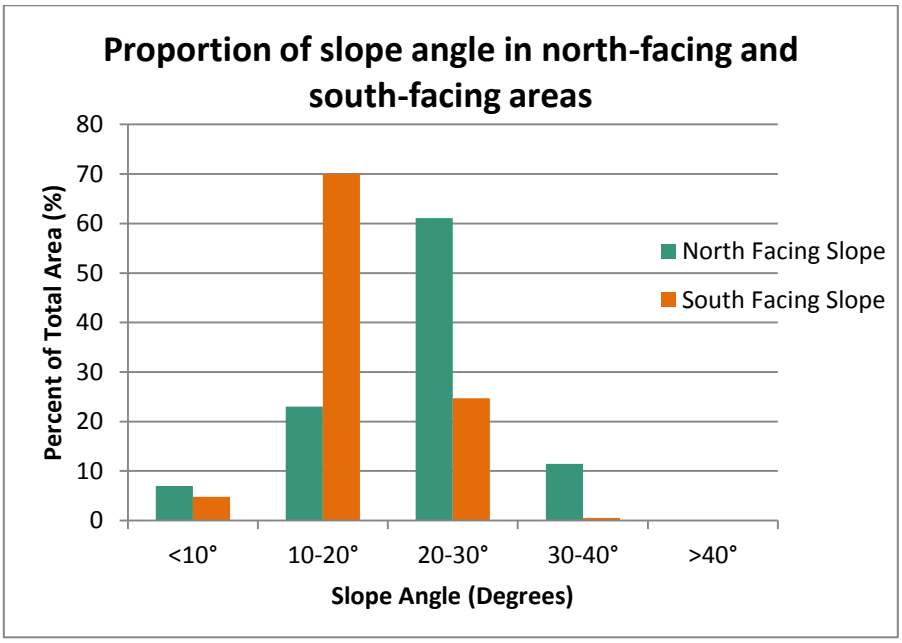

Figure 2-4. Slope steepness surrounding paired stations in Johnston Draw.

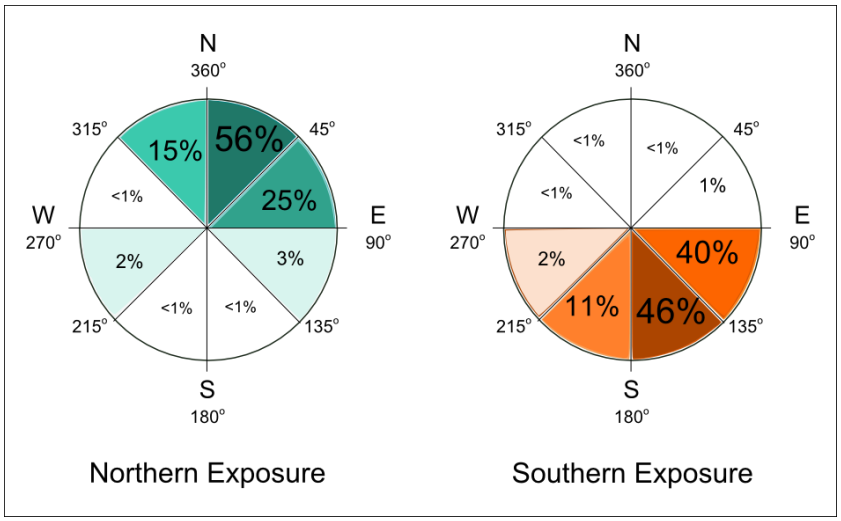

Figure 2-5. Proportion of each slope facing different aspects.

To assess the potential radiation differences between the slopes, a general radiation model in ArcGIS 10 estimated solar radiation based on topography, Julian day, and calculations for global, direct, and diffuse radiation. The model was run for each month of 2012 on the north- and south-facing slopes outlined for terrain analysis (Figure 2-3). No adjustments were made for canopy differences on opposing slopes. The output in Figure 2-6 is the mean monthly solar radiation (W/m^2) for each aspect. According to the GIS model, SFS averages exceed NFS by more than 1300 W/m^2 in the spring (February, March and April) and late summer/fall (August, September, and October). The remaining months of the year solar radiation differences between opposing slopes ranges between 700 and 1000 $W/25m^2$. Minimum monthly solar radiation values on SFS were similar in magnitude to the maximum values on NFS. Although the model output is based on default parameters and does not incorporate canopy structure, results indicate that topography, and corresponding differences in solar inclination angle, have a significant impact on the amount of shortwave radiation energy received by opposing slopes in this watershed.

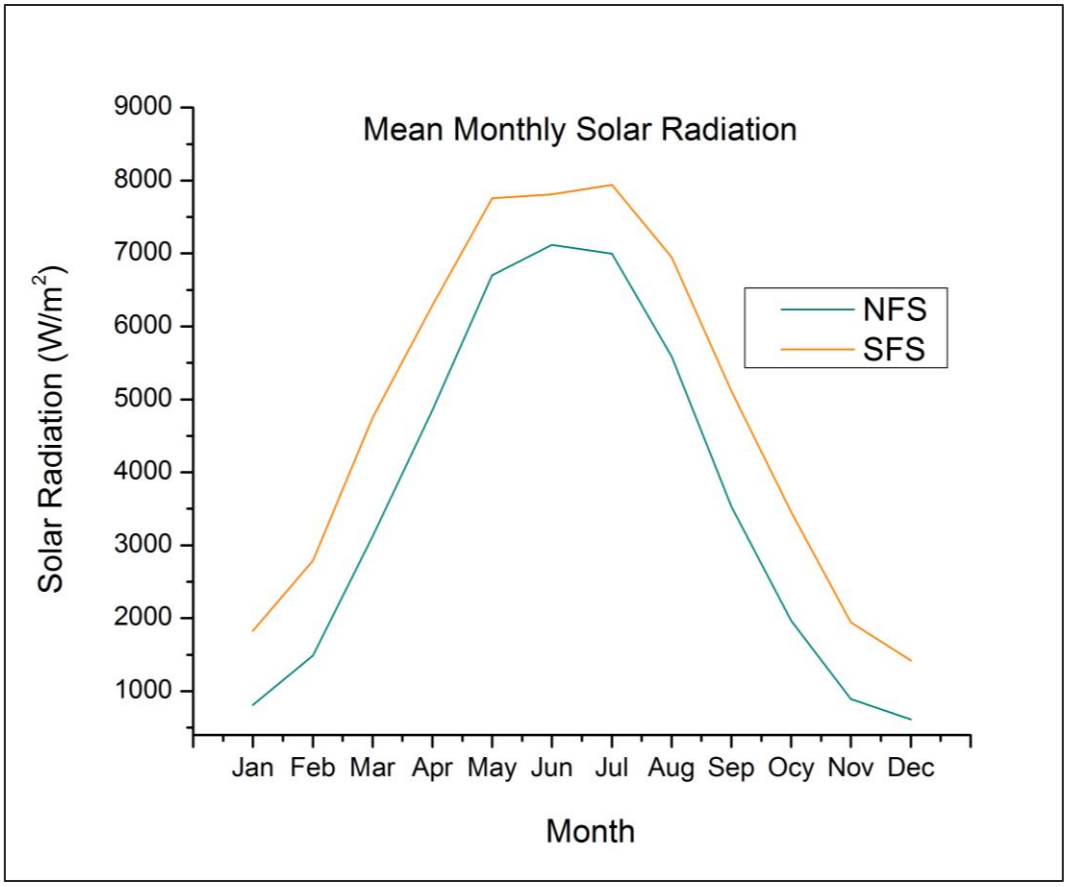

Figure 2-6. Modeled clear sky monthly solar radiation (W/ m^2) on opposing slopes in Johnston Draw.

2.2 Measurements

To quantify the hydrometeorology throughout the watershed, instrument clusters were established in Johnston Draw, both along an elevation transect and at similar elevations on opposing aspects (Figure 2-1). Precipitation measurements, using shielded and unshielded Belfort gauges, date back to 1962 at station 124 and are on-going. Other instrumentation has been added more recently, dating from 2002 to 2011. Stations 124, 124b, and 125 are permanent instrument clusters that measure precipitation, horizontal wind speed (Met-One 034B), air temperature and vapor pressure (Viasala HMP45C), snow depth (Judd UDG), and solar radiation (Eppley PSP). More temporary tripod instrument clusters have been installed at an elevation gradient along the north-facing and south-facing slopes of the watershed. These instrument clusters measure the same hydrometeorological variables as the permanent stations with the exception of precipitation and solar radiation. Table 2.1 lists the instrument clusters by station, location, elevation, and parameters measured. Meteorological data date back to the mid-2000's at stations 124, 124b, 125, 1, 2, 3, 4, and 5 and in 2010 at stations 2b, 3b, and 4b. In addition to surface measurements, soil moisture and soil temperature are measured at multiple depths (5, 20, 35, 50, 75, 90, 100 cm) in profile at stations 1, 2, 3, 4, 2b, 3b, 4b, and 124b using Stevens Hydra Probe SDI-12 soil water sensors (Stevens Water Monitoring Systems Inc., 2007). The Hydra Probes measures the soil dielectric permittivity which is related to soil water content using calibration equations developed by Seyfried et al. (2005) and found to be effective for soils in the area. Two soil profiles located near station 124b are in different vegetation environments, one in mountain sagebrush (124bs) and one in an aspen grove (124ba). All Hydra Probe sensors were installed fall of 2010 at various depths according to soil depth and obstacles encountered at each site. Table 2.2 lists the location and depth of Hydra Probe sensors in the basin. Near the mouth of Johnston Draw a drop box weir, stilling well, and potentiometer gauge streamflow. Discharge is calculated from this data by personnel at the Northwest Watershed Research Center (NWRC) in Boise, ID. See Pierson et al. (2001) for description of drop box weir and data collection methods.

Table 2-1. Location, elevation, and measured parameters at instrument clusters in Johnston Draw.

Installation Type	Station ID	Easting, Northing (NAD27)	Elevation (m)	Precipitation (shielded)	Precipitation (unshielded)	Solar Radiation	Horizontal Wind Speed	Air Temperature	Vapor Pressure	Snow Depth	Soil Temperature	Soil Moisture
Permanent Instrument Cluster	*124*	516395, 4774980	1804	●	●	●	●	●	●	●		
	124b	516622, 4774905	1778	●		●	●	●	●	●	●●	●●
	125	518266, 4774328	1508	●	●	●	●	●	●	●		
Tripod Instrument Cluster	1	518021, 4774221	1548					●	●	●	●	●
	2	517747, 4774287	1604					●	●	●	●	●
	3	517525, 4774169	1655				●	●	●	●	●	●
	4	517326, 4774136	1706					●	●	●	●	●
	5	516776, 4774584	1757					●	●	●		
	2b	517750, 4774610	1611				●	●	●	●	●	●
	3b	517522, 4774592	1659				●	●	●	●	●	●
	4b	517324, 4774664	1704				●	●	●	●	●	●

Table 2-2. Automated soil moisture and soil temperature depths in Johnston Draw soil profiles.

	Soil Moisture / Soil Temperature Measurement Depths								
Station	5 cm	20 cm	35 cm	50 cm	75 cm	90 cm	100 cm	130 cm	190 cm
124ba	●	●		●	●	●			
124bs	●	●		●					
1	●	●		●		●		●	●
2	●	●		●	●		●		
3	●	●		●	●		●		
4	●	●		●	●		●		
2b	●	●	●	●	●				
3b	●	●	●	●					
4b	●	●	●	●					

The instrument clusters in Johnston Draw automatically record measurements every 15 minutes. Although the stations are strategically placed along an elevation gradient mid-slope on opposing slope aspects, they measure these variables at a single point. Additional field data was collected during the snow-free season to determine the representativeness of these points to the surrounding hill slope in snow free months. Soil temperature and soil moisture were measured at 30 cm depths using a temperature probe (Omega Engineering HH806AU, THSS-18G-RSC-12) and Soil Moisture Mini Trase TDR (time-domain reflectometer) (Jones et al., 2002). Ideally, the manual measurements would coincide with depth increments of the automated sensors (e.g. 5 cm, 20 cm, or 50 cm), but excavating soil pits across a hill slope to measure soil moisture would have been impractical both physically and economically. To obtain information for estimating hill slope variability, we opted for periodic extensive sampling surrounding the automated stations and used vertical probes. Since we were interested in more than just the conditions near the soil surface, we chose to measure soil moisture between 0-30 cm, assuming that the variability between 0 and 30 cm would be similar to that of the individual automated depth increments. Although the manual readings would not be directly comparable to the automated profiles, the variability of the manual readings and how closely they were bounded by the data at the automated sites would be informative. For soil temperature, we wanted to make measurements deep enough to avoid strong diurnal fluctuations and reduce the impact of taking measurements at different times of day on multiple visits. Most 30 cm soil temperature data show little or no diurnal fluctuation. Since the soil moisture measurements left 30 cm deep holes, we took soil temperature measurements at 30 cm depth, expecting the values to be bound by 20 cm and 50 cm readings from automated sensors.

Field measurements were made at points spaced 10 m apart in a spatial grid surrounding stations 2, 4, 2b, and 4b. Each measurement grid consisted of 10 points on a north-south trending line and 10 points on an east-west trending line, centered on an instrument cluster station. The result was field measurements spanning 50 m in each cardinal direction from the corresponding station (Figure 2-1). An additional 3 points were measured near the soil profile to assess automated sensors. Field measurements were taken approximately monthly from June-August, 2011, and April-September, 2012.

At the conclusion of field measurements in 2012, soil pits were dug at stations 2, 2b, 4, and 4b to a depth of either 70 cm or resistance, whichever came first. The soil profiles were characterized by layer in situ according to changes in color, structure, and rupture resistance.

Samples of each layer were later processed for particle size using the hydrometer method (Gee and Bauder, 1986).

Chapter 3. Results

Data gathered for this investigation span a range of elevation and slope exposures within the Johnston Draw watershed. To evaluate the relationship between complex terrain and streamflow generation, the data were examined in a step-wise process scaling up in both space and time. In section 3.1, the soil samples are summarized with a basic description of layers, depth, and particle size distribution. Section 3.2 compares automated point measurements to manually collected field data to determine how the single point data relate to the surrounding hill slope and the variability of soil moisture and soil temperature throughout the warmer months within 1000 m^2 areas. From this information, section 3.3 characterizes the variation of snow depth, soil temperature, and soil moisture by elevation and slope exposure within the catchment. Then in section 3.4, individual streamflow generating events are examined over the course of two water years to better understand how snow depth, soil temperature, and soil moisture couple in relation to antecedent and event conditions.

3.1 Soil Characteristics

The soils sampled at stations 2, 4, 2b, and 4b, indicated slight variation among aspect and elevation (Appendix A). Most notably, the soil depths on opposing aspects at stations 4 and 4b were very different in terms of depth. During periodic field measurements, soils surrounding station 4b were observed to be quite rocky in the top 30 cm. When the Hydra Probes were installed, an argillic horizon and soil formation was observed in areas below 50 cm. However, when the soil pit was excavated nearby, the soil layer extended only 35 cm before reaching decaying bedrock. Based on the wavy horizon transition observed between the Cr and R horizons, soil layer depth likely fluctuates as much as 10-15 cm across a single square meter in the vicinity of station 4b. In contrast, the excavation of soils at station 4 extended 100 cm before reaching bedrock during Hydra Probe installation. Later excavation of a soil pit near station 4 was abandoned at 75 cm depth, well before bedrock contact, due to uniformity of the deeper soil layers. Both the 4 and 4b soils classified as loamy sands with the primary difference being percent gravel. Stations 2, 2b, and 4b had approximately 19-22% gravel, earning the modifier *gravelly* when describing texture class (Appendix A, Table A-5), whereas station 4 contained less than 10% gravel per volume. The

soil at station 2b contained much higher clay content than the other sites, averaging 18% per volume. In contrast, soils at stations 4b, 2, and 4 contained 3.8%, 3.1%, and 0.5% clay respectively. In general, soil depths were observed to be deeper on NFS than SFS, and soil texture was very similar for stations 2, 4, and 4b. Notable exceptions were extremely shallow soils at station 4b and much finer earth fraction at station 2b. These findings are similar to soil series descriptions where the Ola series (NFS) is described to be approximately 1 m deep with virtually no profile development and the Takeuchi series (SFS) is more shallow, extending approximately 60 m with a more developed B horizon and more rocky phases (Figure 2-2).

3.2 Upscaling automated point measurements

Figures 3.1 and 3.2 show that automated measurements of soil moisture and soil temperature at 5 cm, 20cm, and 50cm depth generally fall between the minimum and maximum values measured manually. When examining soil moisture values, water contents between 0-30 cm were within one standard deviation of the automated water content recorded at 5 cm, but were different by more than two standard deviations from the 20 cm value, with the exception of station 4 (Figure 3.1). For soil temperature values, manually measured soil temperatures at 30 cm depth were less than one half standard deviation of the automated measurements at 20 cm depth, (Figure 3.2).

Manual measurements of soil moisture and soil temperature provide some insight into the variability of these parameters within 100 meters of slope area. The coefficient of variation was calculated to compare soil moisture to soil temperature. Soil temperatures were remarkably consistent over short distances with very little variability on respective aspects (Figure 3-2). The average coefficients of variation for manually measured soil temperatures at 30 cm depth were 0.10 on NFS and 0.08 on SFS Manually measured soil moisture values, representing 0 to 30 cm depth, were more variable than soil temperatures across the same spatial scale with average coefficients of variation of 0.21 on the NFS and 0.34 on the SFS. In comparing manual soil moisture measurements by aspect, water content in the top 30 cm of soil was observed to be 1.6 times more variable on SFS than NFS (Figure 3-1).

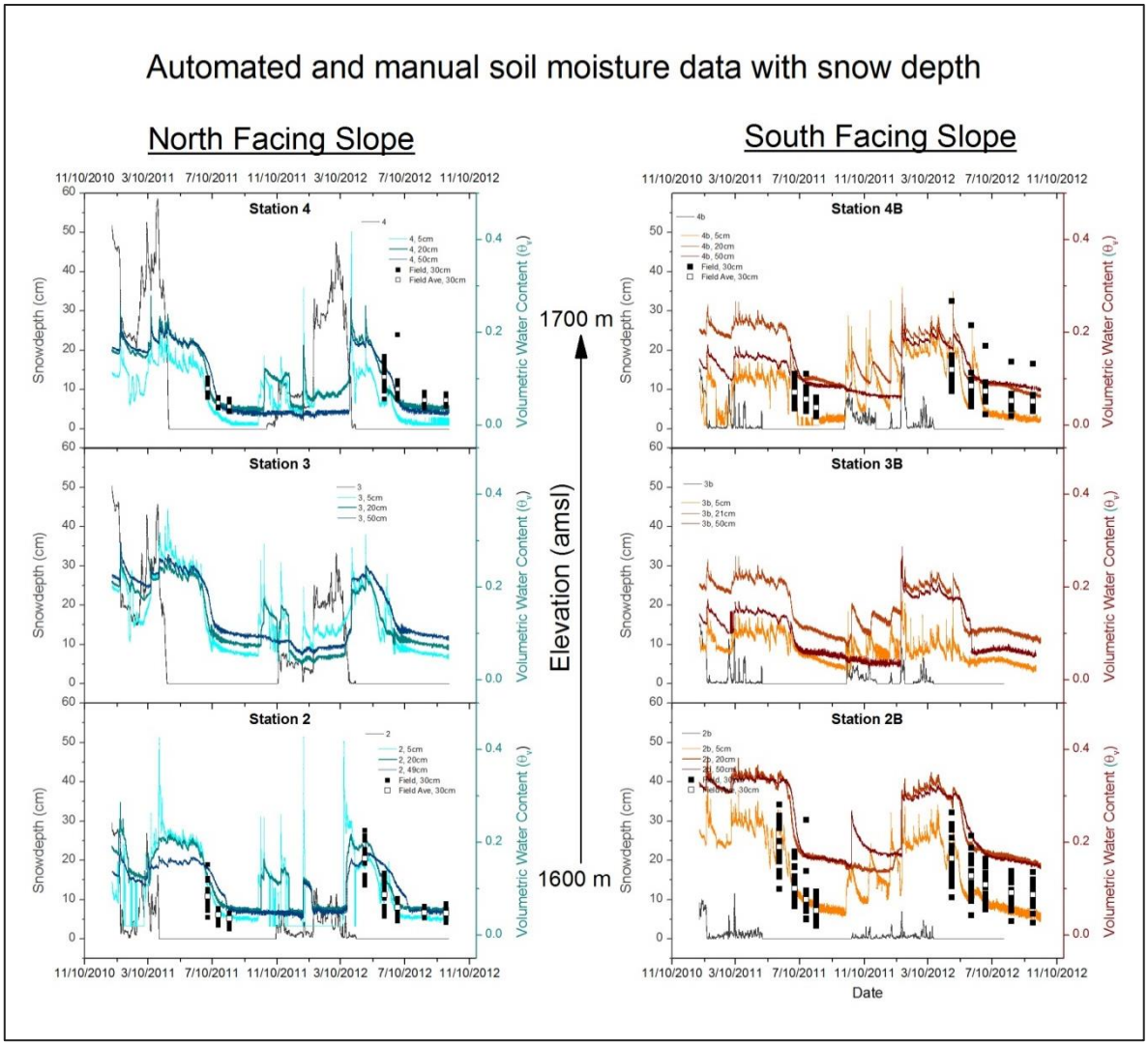

Figure 3-1. Manual soil moisture measurements (black squares) and mean soil temperature (white squares) from 0 to 30 cm depth plotted with automated soil moisture measurements at 5 cm, 20 cm, and 50 cm depth.

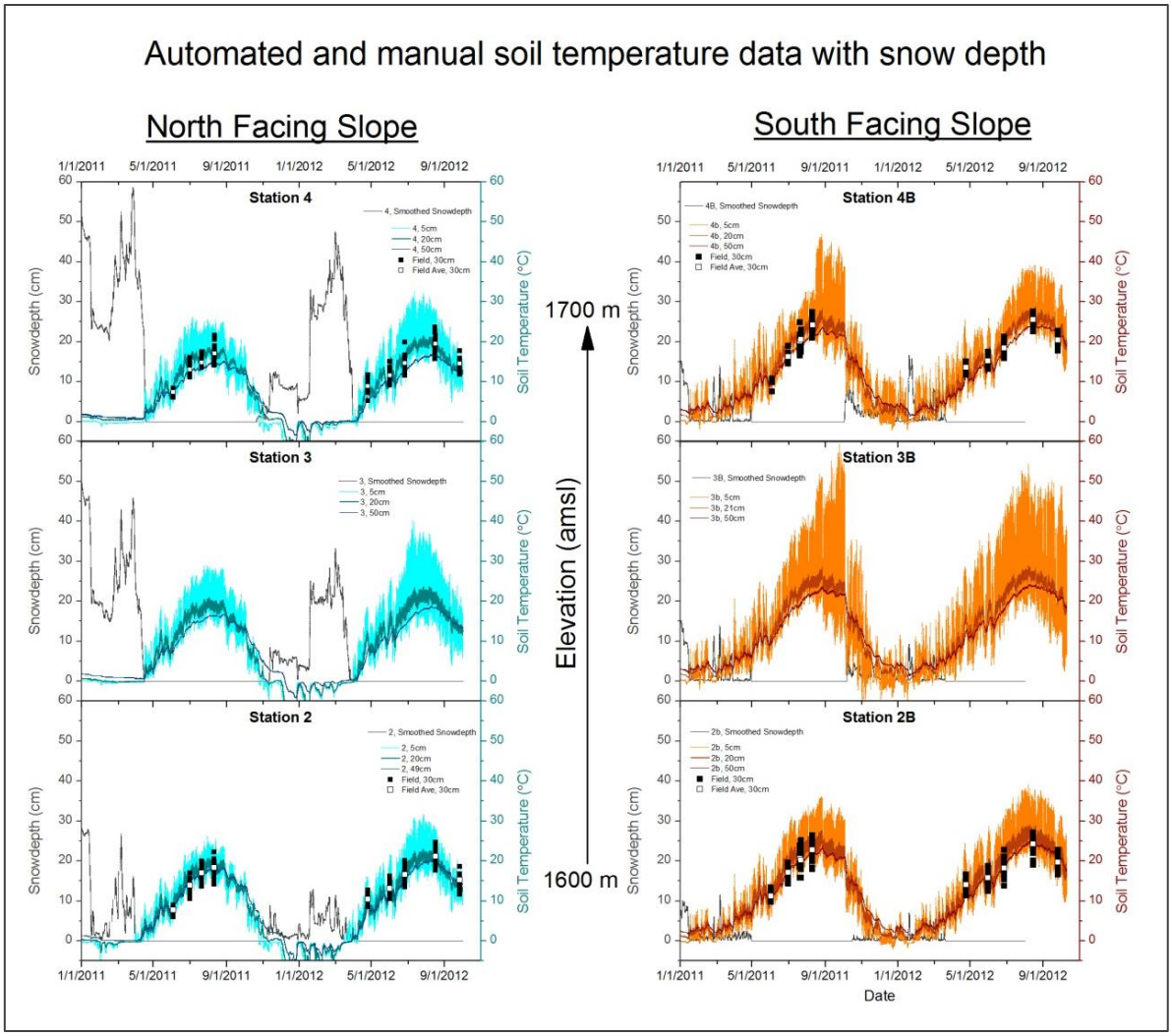

Figure 3-2. Manual soil temperature measurements (black squares) and mean soil temperature (white squares) at 30 cm depth plotted with automated soil temperature measurements at 5cm, 20cm, and 50cm depth.

Manually measured soil temperatures are significantly higher on the SFS than NFS at the 95% confidence interval. However, there is no significant difference indicated at the 95% confidence interval for the 100 meter elevation differences on respective aspects (Figure 3.3(a)). These results indicate that automated soil temperatures exhibit little sensitivity to the 100 m elevation difference relative to aspect and hence could be averaged to quantitatively compare one slope to the other. In contrast to soil temperature, manually measured soil moisture is not significantly different on opposing aspects at the 95% confidence interval with the exception of

values at station 2b, where volumetric water content is approximately twice that of the other locations (Figure 3.3(b)). Therefore, automated water content could not be averaged across the 100 m elevation gradient for each opposing aspect due to the outlier data from station 2b.

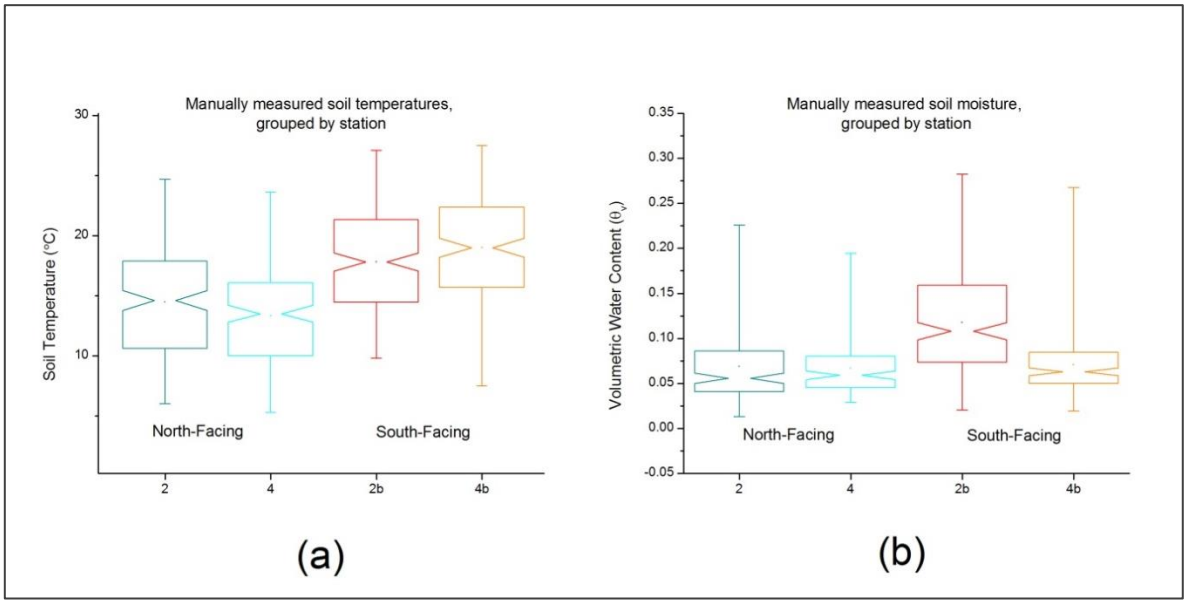

Figure 3-3. Manually measured soil temperature (a) and soil moisture (b) by station. Notches within boxes indicate the upper and lower 95% confidence interval for each dataset.

3.3 Dynamics of hydrologic states and fluxes in complex terrain

3.3.1 Snow Cover

Examination of air temperature, precipitation, and snow depth data indicates that Johnston Draw spans the rain-snow transition zone and experiences frequent snowfall, rain, or rain-on-snow events throughout the cold season (Figures 3-1 and 3-2, Appendix B). Measurements from automated meteorological stations throughout the basin indicate that snow cover is deeper, and more persistent both at higher elevations in the watershed and also at lower elevations on NFS versus SFS (Table 3-1). Over the course of two winter seasons, snow depth between 1600 and 1700 meters elevation was approximately twice as deep on NFS, with an average maximum depth

between 0.3 and 0.6 meters for all sites. The snowpack on NFS persisted seasonally, dampening the near-surface soil temperature fluctuations and maintaining a value near 0°C for 2-3 months (Figure 3.2). In contrast, the SFS were characterized by a transient snow pack that typically lasted for no more than 1-2 weeks and reached maximum depths of only 0.15 meters. Frequent snow melt and shallow snow depths on the south-facing aspect between 1600 and 1700 meters had a minimal effect on diurnal temperature fluctuations near the surface in sharp contrast to the NFS (Figure 3.2). As a result, soil temperatures were more variable during winter months on SFS.

Table 3-1. Snow cover depth and duration throughout Johnston Draw for 2011 and 2012.

			2011		2012	
Station	Elevation (m)*	Aspect	Maximum Snow Depth (cm)	Maximum Snowcover Duration (days)	Maximum Snow Depth (cm)	Maximum Snowcover Duration (days)
125	1500	flat	20	>90	10	60
1	1550	northeast	50	>90	26	65
2	1600	north	28	>90	17	60
3	1650	north	48	>105	35	90
4	1700	north	60	>105	47	90
5	1750	southeast	27	42	37	60
124b	1775	southeast	54	>105	52	70
124	1800	flat	23	>90	17	60
2b	1600	south	16	15	8	13
3b	1650	southeast	15	20	14	10
4b	1700	south	16	15	19	10

* Elevation rounded to nearest quartile

In addition to snow depth variation by aspect, snow depths in the watershed also varied by elevation. On the NFS, between 1600 and 1700 meters, snow depth followed a classic elevation gradient where increasing elevation correlated to increased snow depths. However, the pattern ceased immediately above and below these elevations with deep snow accumulation at station 1 (1550 m) and shallower snow cover at station 5 (1750 m). Snow cover on SFS between 1600 and 1700 meters was homogeneous in 2011 and proportional to elevation gradient in 2012. At the higher elevations (1750-1800 m) snow accumulation was extremely variable with maximum accumulation at station 124b twice that of nearby stations 5 and 124. These higher elevation sites

are characterized by lower relief terrain and likely experience greater snow drifting and redistribution than the lower elevation sites. In Johnston Draw, the correlation of increasing snow depth with elevation was only relevant between 1600 and 1700 meters and did not apply to the lowest and highest elevation regions of the watershed, indicating much greater spatial variability of snow distribution than can be described by elevation alone.

3.3.2 Soil Temperature

Soil temperatures were consistently higher on SFS than NFS throughout the year. Figure 3.6 shows mean daily soil temperature at 5 cm, 20 cm, and 50 cm depth, averaged across the slope for opposing aspects. Soil temperatures on south-facing slopes exceed those on north-facing slopes at all three depths. Annual average soil temperatures of 5cm, 20cm, and 50cm depths are 6.0 °C, 5.7 °C, and 5.2 °C greater on SFS than NFS (Table 3-2). Daily minimum and daily maximum temperatures on SFS also exceed those on NFS by a similar magnitude. Daily minimum temperatures are 4.3 °C, 5.4 °C, and 5.2 °C higher on SFS at 5cm, 20cm, and 50cm depths respectively. Daily maximum temperatures at 5cm, 20cm, and 50cm depths are 9.6 °C, 6.2 °C, and 5.2 °C higher annually (Table 3-2). The daily range of soil temperatures is also higher on south-facing slopes than north-facing slopes, with the greatest difference occurring near the surface (5.3 °C at 5 cm depth) and decreasing deeper in the soil profile (0.1°C at 50 cm depth). As expected, the range between temperature minimum and maximum decreases with soil depth, but even at 50 cm depth, SFS soils are warmer year round and experience greater diurnal temperature fluctuation than NFS soils.

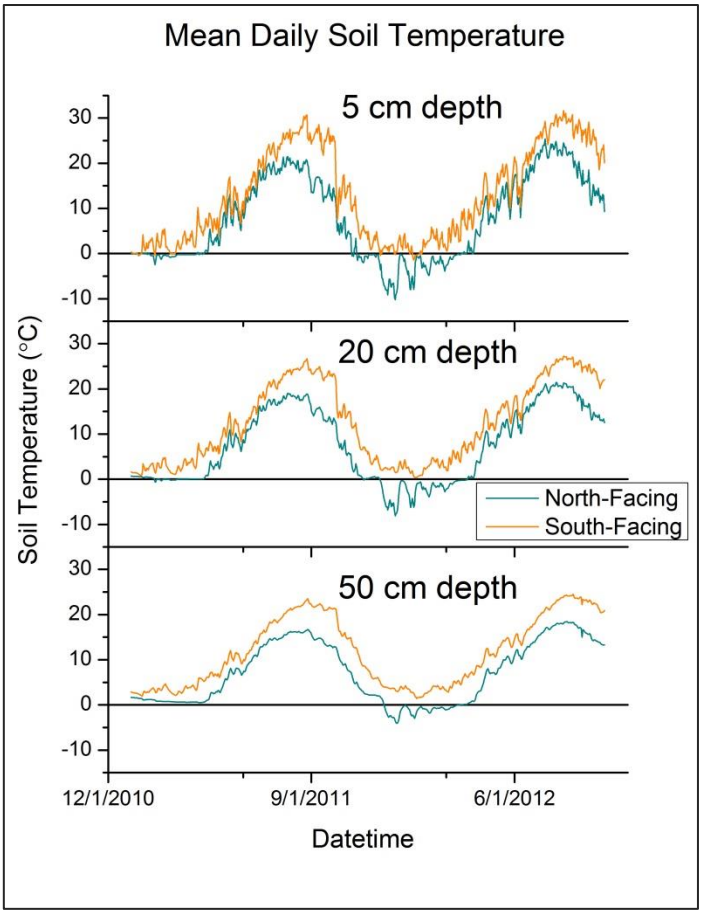

Figure 3-4. Mean Daily Soil Temperatures averaged across opposing aspects for multiple soil depths. At all depths, soil temperatures on the SFS exceed those of the NFS.

Table 3-2. Difference in soil temperatures on opposing aspects.

Mean Daily Soil Temperatures on Opposing Aspects for WY2012				
Metric	Soil Depth	NFS (°C)	SFS (°C)	Temp difference [SFS minus NFS] (°C)
Average Daily Soil Temperature (i.e. Annual Average Soil Temperature)	5 cm	7.0	13.0	6.0
	20 cm	6.9	12.6	5.7
	50 cm	6.9	12.1	5.2
Average Daily Minimum Soil Temperature	5 cm	4.1	8.5	4.3
	20 cm	6.2	11.6	5.4
	50 cm	6.7	11.9	5.2
Average Daily Maximum Soil Temperature	5 cm	10.4	20.0	9.6
	20 cm	7.6	13.8	6.2
	50 cm	7.0	12.2	5.2
Average Daily Range (max-min) Soil Temperature	5 cm	6.3	11.6	5.3
	20 cm	1.4	2.2	0.8
	50 cm	0.3	0.4	0.1
NFS includes stations 2, 3, and 4 SFS includes stations 2b, 3b, and 4b				

3.3.3 Soil Moisture

Due to diifferences in soil properties and a much finer soil texture at station 2b, comparing the total amount of soil water content between sites is inconclusive. However, the transitions, or changes in water storage, reveal similarities among slope aspects and between upper and lower elevations. Soil water dynamics indicated little sensitivity to precipitation phase and timing compared to seasonal evapotranspiration demands in the watershed, as shown by a lack of soil moisture fluctuations in March and April (2011 and 2012) in Figure 3.5. In late fall and early winter, precipitation events infiltrated and began to replenish the soil water deficit from the preceding summer. Vegetation was dormant (visual observation) and hence evapotranspiration should have been at a minimum. Throughout the cold season, precipitation and melt events resulted in additional inputs to soil moisture, as shown by Figure 3.5 (January through March, both years). There was some offset in the timing of soil wetting during the cooler months between NFS and SFS depending on the phase of precipitation and antecedent snow cover and soil temperatures (Appendix C, Figures C-2 and C-4). Since electronic soil water sensors in general are inaccurate

when some part of the soil water is ice, frozen soil conditions cause gaps in the soil moisture curve. This unfortunately was the case during the cooler months, and definitive timing of soil wetting could not be detected due to partially frozen conditions. Generally during the cold season, it appears that soil water storage increased throughout the basin in response to precipitation and melt events. Between January and March, 2012, frozen soil conditions on the north-facing side prevented accurate measurements of water content and it was not until soil temperatures rose above freezing in mid-March that the data could once again be compared to other sites in the watershed (Figure 3-5).

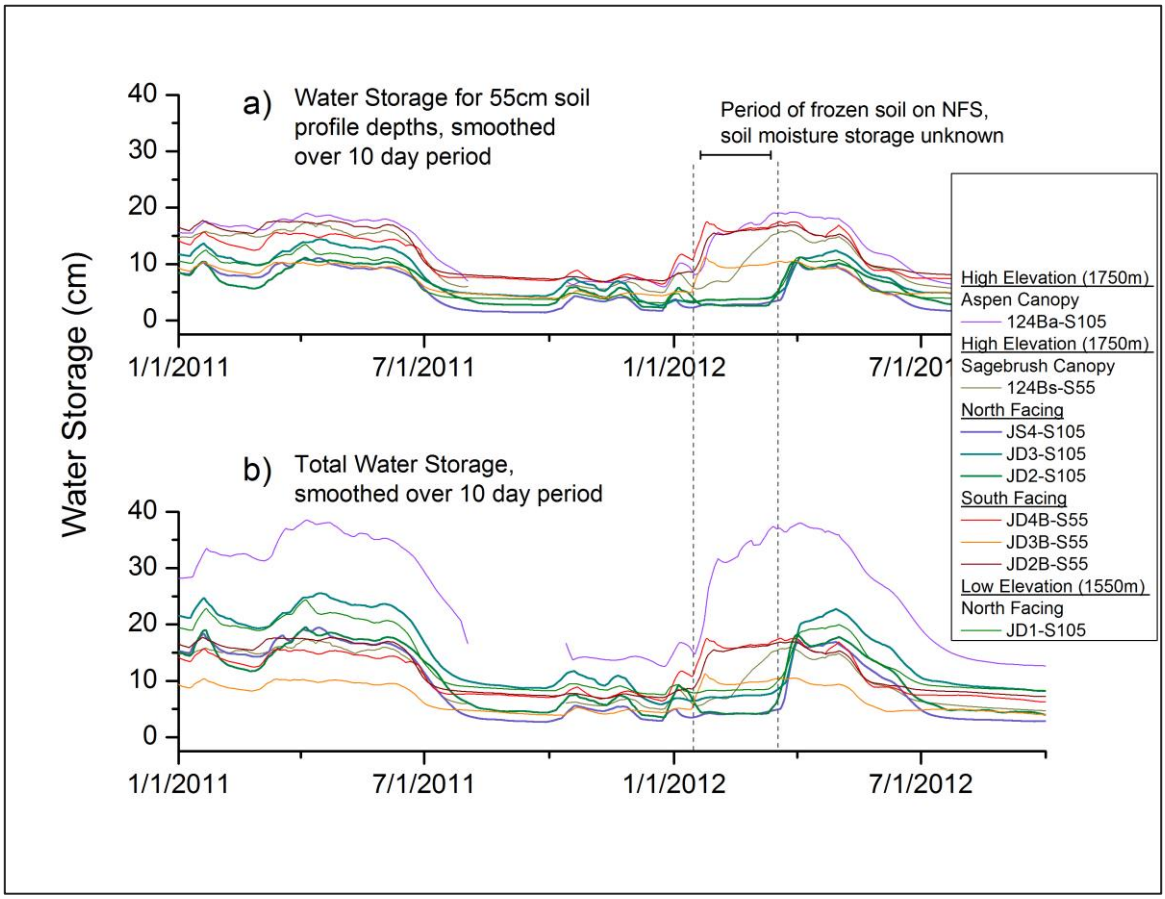

Figure 3-5. Water storage (cm) in the top 55 cm of soil (a) and the total water stored at each site (b) where soils on the NFS and in the high elevation aspen area are twice as deep (~ 1 m) than the shallower SFS soils (~0.5 m).

During the warmer months, soil moisture transitioned from maximum soil water content following spring snowmelt to minimum soil water content in mid- to late- summer. This change in soil moisture content is referred to as a transitional drying period. The transitional drying period is bound by two inflections in the soil moisture curve and defined by the day of year in which the inflections were observed (e.g. January 1, 2011 is day 1). For both water years examined, total water storage reached maximum levels in April, just after seasonal snowmelt and prior to the onset of warm season evapotranspiration. In 2011, the transitional drying period began around day 154; with station 4 beginning to dry down as early as day 152 and station 4b as late as day 159 (Table 3-3). In 2012, the transitional drying period began nearly simultaneously throughout the watershed around day 120, which was nearly one month earlier than observed in 2011.

When soil moisture levels reach minimum, another inflection in the soil moisture curve marks the shift from transitional drying to a summer dry period. For calendar year 2011, this occurred around day 200 for the SFS and as late as day 227 on NFS, almost one month later. In 2012, soils reached minimum water content between day 158 (station 3b) and day 244 (station 124ba). Generally, the high elevation sites and NFS had a longer transitional drying period that extended between 14-80 days further into the summer months in 2012, with the average length of the transitional drying period in 2012 lasting approximately one month longer on NFS than SFS. For both years observed, water stored on NFS remained available for evapotranspiration for approximately one month beyond the time that SFS had reached minimum soil moisture levels.

Table 3-3. Transition timing of soil moisture states following spring wet, high-flux period. Day of year begins on January 1.

			2011				2012			
Soil Depth	Site	Aspect/ Elevation	Begin Transitional Drying Period (day of year)	Water Content* (cm)	Begin Dry Period (day of year)	Water Content* (cm)	Begin Transitional Drying Period (day of year)	Water Content* (cm)	Begin Dry Period (day of year)	Water Content* (cm)
0-55 cm	1	N/1550	155	11.1	205	4	121	10.8	182	4
0-55 cm	2	N/1600	155	10.4	223	3	121	10.2	202	3
0-55 cm	3	N/1650	152	13.1	211	4.9	119	12.4	183	5
0-55 cm	4	N/1700	150	9.4	223	1.6	119	9.7	218	1.6
0-55 cm	124ba	SE/1750	153	18	no data	no data	121	18	215	6.2
0-55 cm	124bs	SE/1750	154	15.9	211	5.6	121	14.9	237	5.2
0-55 cm	2b	S/1600	155	17	199	8.4	121	15.3	186	8.3
0-55 cm	3b	S/1650	158	9.6	199	5.3	121	9.4	158	4.6
0-55 cm	4b	S/1700	159	14.4	200	7.6	121	16.9	179	7.5
1-105 cm	1	N/1550	154	20.7	207	9.1	121	19.9	190	9.2
1-105 cm	2	N/1600	155	17.7	227	5	121	17.8	203	4.8
1-105 cm	3	N/1650	152	23.7	227	9.4	119	22.7	212	9.3
1-105 cm	4	N/1700	152	16.8	229	3.2	119	16.9	201	3.4
1-105 cm	124ba	SE/1750	152	35.3	no data	no data	121	25.9	244	13

*Note water content is representation of continuous smoothing of hourly data over 240 points (10 days)

3.4 Hydrometeorological conditions during runoff generating events

Nine distinct streamflow generating events were identified in the data record between January 1, 2011 and October 1, 2012. Hydrometeorological data throughout the basin surrounding these streamflow generating events are displayed in Appendix C. Climate conditions, changes in snow pack, soil temperatures at 20 cm depth, and soil moisture are summarized by location in the watershed in table 3-4. Individual measurement locations have been grouped together by aspect and elevation to simplify the discussion of runoff generating mechanisms in Johnston Draw. The ridgetop (RT) location refers to station 125 located near the top of the watershed. High elevation (HE) region refers to measurements at stations 124b and 5 and is further differentiated by “HE aspen” and “HE sage” for the soil profile data at station 124b in the aspen grove and sagebrush canopy, respectively. North facing slope (NFS) includes stations 2, 3, and 4 and south facing slope (SFS) includes stations 2b, 3b, and 4b. The lower elevation stations are referred to as a group (LE), or individually when appropriate, as low elevation north (LEN) and low elevation outlet (LEO) for

stations 1 and 125 respectively. Peak flow events are defined by changes in stream stage greater than 2 cm in less than 36 hours.

Because Johnston Draw lies in the elevation range of the rain-snow transition zone, precipitation events frequently transition between rain and snow and often include some mixed-phase events during colder months. For this analysis, the dew point temperature (T_d) was used to estimate precipitation phase, based on the method developed and outlined by Marks et al. (2012) using data from Johnston Draw, where T_d<-0.25°C is 100% snow, T_d>+0.25°C is 100% rain, and -0.25°C<T_d<+0.25°C is mixed rain and snow. Table 3.4 provides a summary of conditions during the nine runoff generating events. A more complete analysis of hydrometeorological conditions is presented in Appendix C, Table C-1.

Table 3-4. Atmospheric, surface, and subsurface conditions during runoff generation events.

Event	**1**	**2.1**	**2.2**	**3**	**4**	**5**	**6**	**7**	**8**	**9**
Event Driver	Midwinter Rain-on-snow	Early Spring Melt	Early Spring Mix Phase Precip	Seasonal Melt	Mix Phase Precip/ Midwinter melt	Midwinter Rain-on-snow	Rain-on-snow/ Midwinter melt	Midwinter melt	Seasonal Melt	Rainfall
Date	1/15-1/16 2011	3/13-3/15 2011	3/15-3/16 2011	3/28-4/1 2011	1/18-1/20 2012	1/20-1/21 2012	1/25-1/26 2012	2/21-2/23 2012	3/2- 4/1 2012	4/26/2012
Radiation % of clearsky	24%	63-72%	45%	57-97%	18-32%	51%	48-68%	35-48%	70% ave	35%
Cloud cover	cloudy	mostly sunny	partly cloudy	mostly sunny	cloudy	partly cloudy	partly cloudy	sunny and cloudy	mostly sunny	cloudy
T_a (°C)	(+) 4-6	(+) 3-4	-1 - +4	0 - +10.5	-1.8 - +2	(+) 2	(+) 2-6	(+) 4-7	-10 - +15 (+3 ave)	(+) 6
T_d (°C)	(+) 0-5.5	(+) 1-3	-0.9 - +3.3	-9.2 - +3.7	-1.2 - +0.5	(+) 0.4-2.5	(+) 0.25-2	-4 - +4	-16 - +6 (-4 ave)	(+) 1-7
e_a (kPa)	0.6 - 0.9	0.4 - 0.7	0.6 - 0.8	0.3 - 0.8	0.4-0.6	0.6-0.7	0.5-0.7	0.4-0.8	0.2-0.9 (0.5 ave)	0.7-0.9
Average Daily Wind Speeds (m/s)	1-11	1.8-7	1.5-7	1-8	2-13	2.5-8	1.5-10	2-13	1-9	2-6
Precip (mm)	3.5	0	2.1	0.4	4.7	3.2	1.6	1	9.6	2.8
Precip phase	rain	na	rain transition to snow	rain	snow; rain and snow	rain	rain	rain	rain and snow	rain
Δ Snow depth (cm)	(-) 5-28	(-) 0.4-10	(-) 0-3.5	(-) 0-24	(+) 6-33	(-) 2.3-4.5	(-) 2-8	(-) 1-12	(-) 5-50	na
Δ Soil Temp at 20 cm depth (°C)	(+) 0-1.8	(+) 0-1	(-) 0-0.6	(+) 0-4.4	(+) 0-5	(+) 0-0.5	Ø	(+) 0-0.8	(+) 1-6	(-) 0.3-1.5
Δ 55 cm Soil Moisture Storage (cm)	(+) 0.3-0.5	(+) 0-0.4	(+) 0-0.1	(+) 0-0.7	(+) 0.4-1.1	(+) 0.2-0.5	(+) 0-1.3	Ø	(+) 0.6-2.6	Ø
Δ Weir Stage (cm)	(+) 4.8	(+) 1.1	(+) 2.8	(+) 2.7	(+) 2.2	(+) 3.6	(+) 3.8	(+) 4.2	(+) 2-4	(+) 2.8

na= not applicable; Ø= no significant change

For this table used daily average of all air temps, average of all vapor pressure, average all daytime radiation, daily average windspeed (no threshold correction); daily average soil temps at 20 cm depth

Event 1: Rain-on-snow driven event

A large rain-on-snow event in early January, 2011 rapidly melted the snowpack and generated peak flows in Johnston Draw and the surrounding Reynolds Creek watershed. The primary rain-on-snow event occurred between January 15, 2011 20:15 and January 16, 2011 19:00 (Appendix C, Figure C-1 and Table C-1). Two days prior to the rain-on-snow, a combination of warm temperatures and precipitation began to melt the snowpack throughout the basin and SFS were completely ablated prior to the large rain event (loss of 7-8 cm snow depth). Air temperature, dew point temperature, and atmospheric vapor pressure all increased to 5.6°C, 5.5°C, and 0.93 kPa respectively (Table 3-4 and Appendix C, Figure C-1). Cloudy conditions reduced shortwave radiation and increased incoming longwave radiation (Table 3-4). Wind speeds in excess of 10 m/s were recorded on the ridgetop and SFS wind speeds (5.6 m/s) were nearly twice the velocities on the NFS and LEO (2-3 m/s). Precipitation was 100% rain, accumulating 3.5 cm during the storm and stream stage increased 4.8 cm over a period of 24 hours (Appendix C, Figure C-1). Streamflow increased slightly during the two days prior, but it was not until the rain event and ablation on the NFS, LE, and HE regions between January 15 and 16 that a distinct peak in streamflow occurred. Due to loss of snow cover on SFS, soil temperatures at 20 cm depth increased to +3.5°C and experienced diurnal fluctuations of 1-2°C. Soil temperatures (20 cm depth) elsewhere in the basin decreased slightly, but the magnitude of change was less than the assumed range of sensor error (± 0.5°C) and therefore soil temperatures were reported as unchanged during this event (Appendix C, Table C-1). Increases in soil moisture storage within the top 55 cm throughout the basin ranged between 0.3-0.5 cm. Deeper soil layers on NFS, HE (aspen site), and LEN indicated soil water increases ranging from 0.6-0.9 cm. In summary, streamflow generation from this rain-on-snow event was due in part to antecedent conditions where warm temperatures and high winds melted the snow pack on SFS and primed snowpack elsewhere in the basin for a midwinter melt, causing a slight increase in stream stage. The primary stream flow peak occurred when the addition of rain was combined with on-going snow melt.

Event 2: Early Spring Melt Event

This event was characterized by snowpack melting followed by a precipitation event that began as rain and transitioned to snow. The first stage of this event occurred between 3/12/11 8:00 and 3/15/11 17:00, during which there was very little cloud cover (63-72% of potential), air and dew point temperatures were 1 to 4°C above freezing, and vapor pressure ranged between 0.4-0.65 kPa (Event 2.1 in table 3-4). Winds increased to 5 m/s on the SFS and approximately 2.5 m/s on the NFS. During this period snow depth decreased between 5-10 cm in HE and RT areas, 5-7 cm on NFS and the remaining snowpack of less than 1 cm was ablated on SFS and LE regions (Appendix C, Figure C-2). Soil temperatures increased slightly (0.5-1°C) on SFS and remained relatively unchanged in HE, NFS, and LEN locations. SFS water content remained relatively unchanged and at NFS and LEN locations, water content in the top 105 cm increased by 0.4-0.5 cm. Stream flow increased during the early spring melt phase, but did not peak until precipitation in the form of rain occurred between 3/15/11 17:00 and 3/16/11 0:00 (Event 2.2, Table 3-4). Clear sky radiation potential decreased from 72% to 45%, indicating partly cloudy conditions. The snow pack, where present, ceased to melt during this period. Around 3/16/11 0:00 both air and dew point temperatures dropped below 0°C, precipitation transitioned to snow, and streamflow began to decline. The rain-snow transition zone moved from the top of the watershed down in elevation over a period of 4-5 hours between 3/15/11 19:30 and 3/16/11 2:30 and snow accumulated at all stations except at the lowest elevation near the outlet (LEO).

During the brief rainfall, soil temperatures remained unchanged beneath the snowpack on the RT, HE, NFS, and LEN areas. SFS soil temperatures decreased 0.6°C in conjunction with decreasing air temperatures and decreased shortwave radiation. Soil moisture content did not change on SFS, regardless of direct precipitation input. Increases in soil water content on NFS, HE, and LEN areas were quite small ranging from 0-0.2 cm. The relatively unchanged soil moisture content coupled with stream flow increase indicates the soil water deficit had been satisfied prior to this event. In summary, streamflow increases coincided with both an initial snowmelt and additional rain input. The rainfall event transitioned to mixed-phase precipitation, leaving snow depth unaffected where snow cover remained in the watershed.

Event 3: Seasonal Melt Driven Event

As the seasons transitioned from late winter to early spring, warm air temperatures and melting snowpack generated peak streamflows. For event 3, primary seasonal melt occurred between 3/28/11 12:00 and 4/1/11 12:00 with complete snow ablation at all locations except NFS stations 3 and 4, and HE station 124b (Appendix C, Figure C-3). These higher elevation/north facing locations retained some snow cover for an additional two weeks, completely ablating between 4/14/11 and 4/16/11 and producing a secondary peak in streamflow. Large shortwave radiation (57-97% of potential) coupled with above-freezing air temperatures and moderate wind speeds contributed to melting the snowpack, which in turn increased streamflow stage by 2.7 cm. Where snow ablated, surface soil temperatures began to rise and fluctuate with diurnal air temperatures. The largest increases in soil temperatures occurred on SFS, followed by LE, and southeast-facing HE areas. Soil moisture neither increased nor decreased on SFS during this period, suggesting the soils were already saturated. Soil water contents on the NFS and HE increased 0.6-1.1 cm in the top 105 cm. Streamflow initially peaked 3/31/11 between 0:00 and 15:45, followed by sustained high flows and multiple minor peaks through 4/3/11 (Appendix C, Figure C-3). A secondary peak was observed around 4/17/11 when a rain event of 1.3 cm coincided with complete ablation of high elevation/north-facing areas. In summary, this seasonal melt correlated with increased shortwave radiation and warm air temperatures. Very little precipitation occurred, indicating the bulk of water input for streamflow came from snow melt throughout the watershed. Large water inputs sustained high streamflow amid multiple peaks in runoff.

Event 4: Simultaneous Mixed Phase Precipitation and Melt Driven Event

In water year 2012, the Johnston Draw channel was dry and early winter snows melted quickly during November and December. Not until 1/18/2012 did snow accumulate throughout the basin and a snowpack become established following 4.7 cm precipitation. The precipitation event began as snowfall at 10:00, transitioned to mixed phase snow and rain between 18:30 and 22:00, and back to snowfall until 1/19/2012 06:00 (Appendix C, Figure C-4). Clear sky radiation potential ranged between 18% and 32%, indicating cloudy conditions. This large storm event resulted in accumulation of 33 cm of snow at HE locations, 11-26 cm on NFS and at LEN, 7-16 cm on SFS, and 6-8 cm in the flat RT and LEO regions (Table 3-4 and Appendix C, Table C-1). The dry channel began to

flow with an initial peak of 3.8 cm stage height. Due to below freezing soil temperatures on the NFS and HE aspen area, soil moisture data were unavailable for these locations. On SFS and the HE sage location, soil moisture increased 0.8-1.1 cm and 1.4 cm, respectively. Although there was some rain mixed with snow during this event, snow depths continued to rise at a steady rate. Despite increases in snow depth throughout the event, streamflow also increased, indicating some water input either by rain, snowmelt, or both.

Prior to the event, soil temperatures were 0.3 to 7 °C below freezing at 5 cm, 20 cm, and 50 cm depth throughout the watershed with the exception of SFS and HE sagebrush locations. The accumulation of snow corresponded with warming soil temperatures near 0°C in NFS, LEN, and HE aspen locations. On SFS, near surface soil temperatures were below freezing (-0.3-1.9°C), 20 cm depth soil temperatures were just above freezing (+0.3-0.6°C), and 50 cm depth soil temperatures were +2-3°C (Appendix C, Figure C-4). During the event, SFS soil temperatures converged towards 0°C but continued to be cooler at the surface (-0.8-0.2°C) and warmer at depth (+0.2-0.5°C at 20cm and +1.6-2.3°C at 50cm). Soil temperatures at the HE sage location trended similarly but were cooler overall by 1-2°C.

In summary, this runoff generating event was a combination of snowmelt and mixed phase precipitation. Mixed phase precipitation contributed to streamflow directly in the form of rain and indirectly as immediately melted snowfall (i.e. delayed rain). Precipitation and snowmelt during this event initiated seasonal streamflow in the dry channel bed.

Event 5: Rain-on-snow Driven Event

Immediately following Event 4, a second, much higher streamflow peak occurred when precipitation fell as rain on the newly accumulated snowpack. The event consisted of 3.2 cm of rainfall between 1/20/2012 12:00 and 1/21/2012 1:00 (Appendix C, Figure C-4). Air and dew point temperatures warmed above freezing to 0.4-2°C, shortwave radiation increased from 18% to 51% of potential, and winds continued at moderate velocities of 2.5-8 m/s (Table 3-4). Snow melt between 2.3 and 4.5 cm was recorded throughout the basin and snow cover at the RT location was completely ablated. Soil temperatures warmed approximately 0.3-0.5°C at RT, HE, NFS, and LE

locations as they converged towards 0°C, with peak soil temperatures stabilizing just below freezing. Due to frozen soil conditions, soil moisture storage on the NFS and at LEN was unknown during this event. For SFS and HE aspen locations, soil moisture increased by 0.5 cm and 0.2 cm, respectively. This rain-on-snow event was smaller than the observed Event 1, but included much the same conditions such as warm air temperatures, moderate winds, and energy input from rain. Runoff was generated by a combination of snowmelt and direct precipitation input.

Event 6: Hybrid Rain-on-snow /Midwinter Melt Driven Event

In January, 2012, a combination of precipitation and snowmelt contributed to peak streamflow. Accumulated precipitation during the event was quite low (1.6 cm) compared to other runoff-generating mid-winter rains that were in excess of 3 cm (Events 1 and 5). The event occurred between 1/25/12 0:00 and 1/26/12 12:00 (Appendix C, Figure C-5). Partly cloudy conditions reduced incoming shortwave radiation to 50 and 60% of potential. Air and dew point temperatures were above freezing (5-6°C and 2°C respectively) and warm winds increased throughout the watershed to 5-8 m/s. Snow melt in the basin ranged between 5-8 cm throughout and the cover was completely ablated at LEO and SFS stations 2b and 3b (Table 3-4 and Appendix C, Table C-1). Soil temperatures were relatively unchanged, warming less than 0.5° C at depth and anywhere snow cover remained. Soil temperatures rose above freezing (+2-4°C) near the surface at stations 2b and 3b in conjunction with complete snowmelt. Due to freezing soil temperatures, soil moisture content was unknown for HE sage and NFS. At the HE aspen location, soil moisture increased 1.3 cm in the top 55 cm of the profile and 2.6 cm in the top 105 cm. Soil moisture on SFS was relatively unchanged during the event. Streamflow generation during this event was a result of snowmelt correlated with a small amount of rain, warm air temperatures, and high winds.

Event 7: Midwinter Melt Driven Event

Events and watershed conditions prior to this midwinter melt contributed to the available water for runoff during the main event. Immediately preceding the melt and peak runoff event, 1.2 cm of precipitation in the form of snow accumulated throughout the basin. At the LEO location, no snow accumulated, indicating the rain-snow transition line to be somewhere between 1500 and

1550 m. Where bare ground existed on the SFS, soil temperatures were above freezing (+1-4°C). The midwinter melt event occurred between 2/21/12 6:00 and 2/23/12 0:00 (Appendix C, Figure C-6) when air temperatures rose from 0°C at daybreak of 2/21/12 to +6°C near evening fall and stayed warm overnight and the following day (+4-7°C). Light precipitation during the day on 2/21/12 totaled 1 cm. Average daily shortwave radiation values indicated cloudy conditions (35-48% of potential), with a brief period of full sun on 2/22/12 between 9:30 and 12:30 (Table 3-4 and Appendix C, Table C-1). Winds were moderate at LE and NFS locations (2-4 m/s) and high on SFS and RT areas (5-13 m/s). The 1-2 cm of accumulated snow on SFS melted completely and snow depths on NFS decreased by 6-12 cm (Table 3-4). Soil temperatures were relatively unchanged at HE, NFS, and LEN locations due to existing snow cover. Soil temps on the SFS warmed near the surface to 2-3°C and 0.3-0.7°C at 20 cm depth. Soil water content was little changed during this melt event, suggesting antecedent saturation. The only detectable change was an increase of 0.4 cm water stored in the top 105 cm of the HE aspen location. Runoff generation during this event was likely sourced primarily by snowmelt in the basin, with a small amount of input from precipitation.

Event 8: Seasonal Melt Event

This month long event occurred in stages, with multiple sub-events of melt and snow accumulation contributing to peak runoff and sustained high stream flows between 3/2/12 12:00 and 4/1/12 0:00. Immediately preceding the event, air and dew point temperatures were below freezing for several days, conditions were partly cloudy, and 1 cm of precipitation fell as snow, establishing snow cover throughout the watershed. At the onset of the event, freezing air temperatures rose to +6°C and shortwave radiation was near maximum, averaging 93% of potential. Snow began to melt throughout the basin and was completely ablated by 3/4/12 2:00 at LEO, and SFS. This cycle of snow accumulation and melt occurred five more times during the month, with the final two cycles consisting of mixed phase precipitation and an upwards migrating rain-snow transition elevation. Each precipitation/melt cycle contributed to a pulse in stream runoff amidst a strong diurnal streamflow pattern (Appendix C, Figure C-7). Values presented in table 3-4 (and Appendix C, Table C-1) represent the general range for the entire seasonal melt period and therefore do not capture the details of these sub-event cycles.

Over the course of the seasonal melt event, a total of 9.6 cm of precipitation fell in the watershed. Air temperatures ranged from -10°C to +15°C and averaged +3°C. Vapor pressure and dew point temperatures were also quite variable, averaging 0.5 kPa and -4°C respectively. Occasional wind gusts occurred, but generally winds were light to moderate with an average of 6 m/s on the ridge, and 3 m/s on opposing slopes and low elevations. Soil temperatures were below freezing on the NFS and at the LEN location until snow cover was completely ablated during the last few days of March so changes in soil moisture were indeterminate for these locations. At the HE locations (both aspen and sagebrush) soil moisture increased by 2.1-2.6 cm and soil moisture on SFS increased 0.6-0.9 cm in the top 55 cm. The deep soils at the HE aspen location increased a total of 3.8 cm in the top 105 cm. Soil temperatures increased 5-6°C on SFS and at HE sagebrush and LE locations and 1-4°C on NFS and at the HE aspen location. Snow melt and precipitation contributed to runoff and maintenance of high flows throughout this event. Overall, the combination of precipitation and larger amounts of water stored as snowpack on NFS and HE locations indicate that much of the runoff was generated from these areas during this event. This melt event was similar to the 2011 seasonal melt (Event 3) in that snowmelt was correlated with increased shortwave radiation, calm atmospheric conditions, and warm air temperatures rather than cloudy conditions coupled with high warm winds characterizing many midwinter melt events (e.g. Events 1,5,6, and 7).

Event 9: Rainfall Event

Soon after the seasonal ablation, the watershed was affected by a moderate rainfall event. Since recent water inputs had satisfied the soil moisture deficit, soils were primed for generating a streamflow peak. On April 26, 2012, 2.8 cm of rain fell over a period of 15 hours and stream stage increased 2.8 cm (Appendix C, Figure C-8). Atmospheric conditions were cloudy (35%) with light to moderate winds (3-6 m/s) and warm air temperatures averaging 6°C (Table 3-4). Dew point temperatures at the beginning of the event were 7°C and fell to 1°C towards the end of the event. Vapor pressure ranged from 0.7 to 0.9 kPa. This event occurred during the high-flux transitional wetting period, following the complete ablation of snow and likely prior to the onset of substantive seasonal transpiration. During the event, soil moisture and soil temperatures remained relatively unchanged. An interesting observation was the absence of measured response in soil moisture,

indicating that soils were relatively saturated at the time of the event and surplus moisture was likely immediately translated to streamflow. This was the only runoff generating event observed during the two year record that did not include mixed phase precipitation or snowmelt.

Chapter 4. Discussion

The data presented illustrate the variability of hydrometeorological dynamics over short distances in complex terrain. Elevation, slope, and aspect dramatically influence snow distribution and melt rates, soil temperature, and water fluxes and storage in the soil profile. By examining the interaction of hydrometeorological parameters across complex terrain, we can better understand how snow, soil temperatures, and soil moisture are coupled in complex terrain environments. The data also enable us to make some inferences of how streamflow is generated throughout the basin and what influence elevation or aspect may have on those runoff generating mechanisms.

4.1 Within-slope variability of soil moisture and temperature during summer months

The manual measurements of soil water content and temperature indicate what level of variability may occur within a short distance (100 m or less) from the automated measuring stations. Soil temperatures were observed to be remarkably consistent, showing very little variation within the 1000 m^2 measurement areas and their respective slope aspects. In contrast, soil moisture values were more variable on SFS than NFS each day the manual measurements were taken. While differences in slope energetics and vegetation certainly contributed to observed soil moisture variability, there were also differences in the soil properties between each station location to consider as well. During the installation of automated Hydra Probe sensors, SFS soils were observed to have an argillic layer at varying depths. Based on automated soil moisture data from station 2b, where this argillic layer is prevalent at 15-20 cm depths, the water holding capacity of the argillic horizon may be nearly twice that of the loamy sand found in the upper horizons of the SFS and throughout the soil on NFS. Evidence of an argillic layer at station 4b was noted during Hydra Probe installation, but was not detected in the automated sensor data. Since the depth, thickness, and location of this argillic layer on the SFS varied, the 30 cm probe used for measuring soil water content likely included this layer at some measurement points and not at others. The increased water storage capacity of the argillic layer would inevitably contribute to more variability

in measured water contents across a slope. Based on the evidence in this dataset, soil temperatures are more easily characterized in space than soil moisture.

4.2 Snow cover and complex terrain

Snow cover in Johnston Draw was observed to be quite variable, with snow depths that did not appear to be directly related to the elevation differences in the watershed. On SFS, snow depth was observed to be highly transient, with accumulated cover lasting only 1-2 weeks and total snow cover depths roughly half that observed on NFS. Snow cover variability throughout the basin was a function of topographic variability, as well as antecedent snow and soil temperature conditions driven by topographic variability, and precipitation timing and phase. For example, at the beginning of the data record, January 1, 2011, snow cover was present throughout the basin. A rain-on-snow event from January 13-16 depleted snow cover on the SFS and soil temperatures rose above 0°C at all depths (Figure 3-2). On NFS, soil temperatures remained near 0°C, and some snow cover was retained. Subsequent snowfall on January 18, 2011 increased snow depths on the NFS and soil moisture storage continued to decline from the previous event peak. On SFS, no new snow accumulated and soil moisture storage continued to increase, indicating that elevated soil temperatures and therefore heat flux likely contributed to melting of the new snow. Due to the antecedent conditions, the January 18, 2011 snowfall event was temporarily stored on NFS whereas it infiltrated into the soil profile on SFS. Furthermore, these contrasting conditions existed throughout the remainder of the cold season, resulting in transient snow cover and shallower snow depths on the south-facing side and flat locations (stations 125 and 124) compared to north-facing locations.

In the 2011/2012 cold season, early winter conditions differed from the previous year, yet snow cover conditions followed similar patterns between NFS and SFS and were influenced by both antecedent snow conditions and soil temperatures. Between November and January (2011/2012), snow cover was transient throughout the basin and frequent ablation events only slightly increased soil moisture storage. Soil temperatures during December (2011) hovered around 0°C on the SFS and fell below freezing on the NFS. A shallow snow cover (less than 2 cm) on NFS did not insulate the soil from sub-freezing air temperatures. Soil temperatures on SFS, in contrast, were warmer

than the average air temperatures despite little to no snow cover. This difference in soil temperatures between the NFS and SFS likely contributed to the variability in snow cover observed when snow began to fall and accumulate in mid-January, 2012. Snow accumulated throughout the basin and was retained as a seasonal snowpack on the NFS and at higher elevations until early April 2012. Lower elevation and south-facing locations retained snow cover for much shorter durations, lasting an average of only 3-6 days (Figure 3-5). Despite different antecedent snow and soil temperature conditions in water year 2012, the relative differences in snow cover depth and residence times between opposing slopes were observed to be quite similar between water years 2011 and 2012.

Snow depth in some areas of the watershed behaved as expected based on slope, aspect, and elevation; however, this did not hold at the broader watershed scale due to the influence of other processes (e.g. drifting). Within the steeper mid-slopes of the lower watershed, snow cover on NFS was twice as deep as that on SFS and persisted for months at a time compared to weeks. Between the elevations of 1600 and 1700 meters, snow cover on opposing aspects followed a respective elevation gradient, with increasing depth corresponding to increasing elevation. However, evidence of the snow depth/elevation gradient was absent elsewhere in the watershed. For example, station 1 (north-facing, 1550 amsl) and station 124b (southeast-facing, 1750 amsl) experienced similar snow cover depth and duration throughout the cooler months, despite being 200 m apart in elevation and on opposing aspects. This evidence indicates that snow cover is variable in Johnston Draw and may not be explained by elevation and aspect alone. Similar observations have been noted in Reynolds Creek (Winstral and Marks, 2002; Winstral et al., 2013). Additional factors influencing snow redistribution and the energy balance of snow dynamics (e.g. snow drifting, terrain structure, vegetation) need to be incorporated in order to better understand the distribution of snow in this complex terrain.

4.3 Soil temperatures and complex terrain

Previous investigations of the relationship between aspect and soil temperature concur with the findings of this study that SFS soil temperatures are an average +5.2°C higher than NFS. Ebel (2012) investigated the effects of slope aspect on soil temperatures in forested mountain

terrain (2400 amsl) following wildfire activity. In unburned areas, south-facing exposures were 5°C warmer and more highly variable than north-facing exposures within the top 30 cm of soil. Following the wildfire, aspect controls on soil temperature were observed to disappear and the primary driver of this effect was determined to be differences in canopy cover and surface litter on opposing aspects. Kang et al. (2000) developed a hybrid model for predicting soil temperature across landscapes and found the model to be highly sensitive to differences in air temperature and leaf area index (LAI). In an effort to develop a simple model based on variables readily available through remote sensing, the authors focused their efforts on relationships with air temperature and LAI and did not account for other factors such as shortwave radiation. In Johnston Draw, warmer soil temperatures observed on south-facing slopes were likely influenced by sparser vegetation cover and surface litter, coupled with transient snow cover, and increased solar radiation. Shallower soils on the south-facing slopes also store less water for transpiration in the warm season, which in turn influences vegetation canopy density and soil temperatures during the warm summer months. In the cooler months, warmer soil temperatures combine with mixed phase precipitation events and increased snow melt, resulting in decreased snow depths and duration. Surprisingly, exposed southern exposure soils during winter months did not fall below freezing except for rare brief occasions and tended to maintain temperature near 0 °C or increase in temperature following snowmelt. In contrast, winter soil temperatures on NFS were usually near 0 °C or well below freezing. Given the fact that vegetation effects are minimal in the winter and the sun angle is lower in the horizon for northern latitudes, warmer soil temperatures during winter months are most likely driven by increased solar radiation on SFS compared to NFS, with some contribution from stored soil heat in the summer months.

Throughout the year, NFS soil temperatures are cooler and less variable than SFS soils. Cooler soil temperatures on NFS in the summer months may be partially attributable to increased canopy cover. Deeper soils on NFS store greater amounts of moisture longer into the season, providing for denser vegetation and longer periods of active transpiration compared to SFS. The increased canopy cover reflects more shortwave radiation and reduces near-surface turbulent flux, in addition to being correlated with increased surface litter which insulates soil from energy input (Ebel, 2012). In the cooler months, snow cover insulates the NFS soils causing the soil temperatures to remain steady near 0°C or below freezing, depending on antecedent conditions. Insulating snow cover and less shortwave radiation in the winter months result in reduced energy

inputs to soils on NFS. The overall effect, as a result of slope angle and aspect, is cooler soil temperatures and less temperature variation throughout the year on NFS when compared to SFS.

To gain perspective on the magnitude of difference in soil temperatures between opposing aspects, average monthly soil temperatures were examined from relatively flat locations in the surrounding Reynolds Creek Experimental Watershed. Figure 4-1 shows average monthly soil temperatures at the same elevation on opposing aspects in Johnston Draw (Stations 3 and 3b, 1650 m) alongside soil temperatures from Reynolds Mountain East at 2100 meters elevation and the Flats location at 1190 meters elevation (Figure 2-1). The south facing site in Johnston Draw has soil temperature similar in magnitude to the low elevation Flats location and the north facing site is closer to average soil temperatures at the high elevation Reynolds Mountain East location. At the same elevation in Johnston Draw, soil temperature differences on the opposing aspects are similar to temperature differences over roughly 900 meters of elevation at level sites in the Reynolds Creek Watershed.

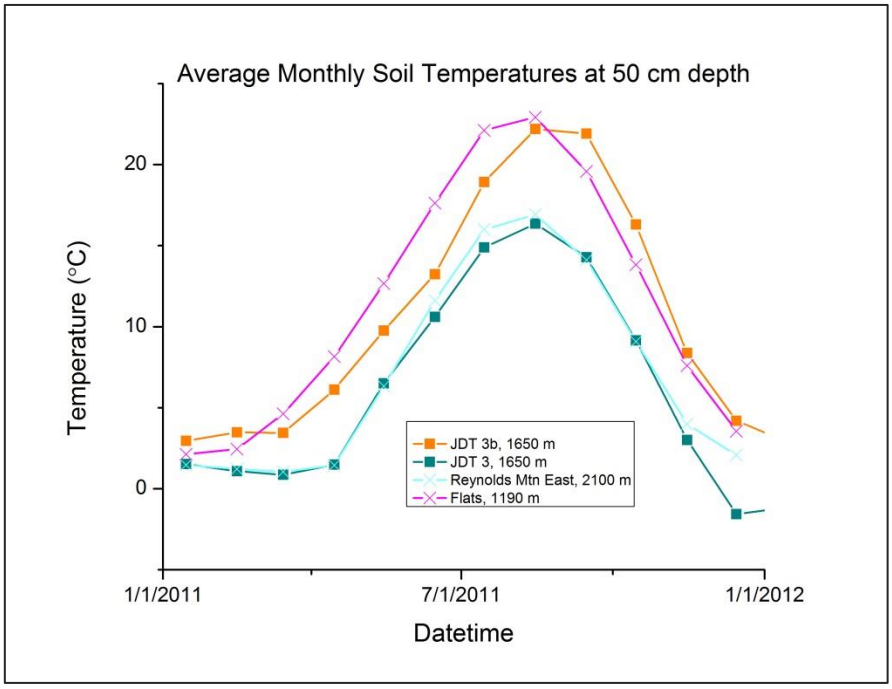

Figure 4-1. Soil temperatures (50 cm depth) on opposing aspects in relation to 900 m elevation change.

4.4 Soil Moisture States (i.e. Hydrologic Seasons)

Soil water storage in Johnston Draw followed a very similar pattern to the soil moisture states described by McNamara et al. (2005) for Dry Creek. However, unlike the Dry Creek study, our analysis did not include modeled evapotranspiration and the timing of each hydrologic season was determined by examining changes in water storage, precipitation, snowmelt, and streamflow. Figure 4.2 illustrates the timing of hydrologic seasons in Johnston Draw for water year 2012. Individual stations were grouped together to represent regions of the watershed as follows: 124ba and 124bs are high elevation; 2, 3, and 4 are north-facing slope; and 2b, 3b, and 4b are south-facing slope. At the beginning of the water year, October 1, 2012, all regions of the watershed were in the summer dry period (Phase I) with low soil moisture content, a dry streambed, and (speculatively) evapotranspiration exceeding precipitation. The transition to a fall wetting period (Phase II) occurred when precipitation likely exceeded evapotranspiration, indicated by the wetting front reaching 20cm or greater depth. In Johnston Draw, the beginning of the fall wetting period was staggered approximately 10 days between different regions of the watershed, and therefore was nearly synchronous. The NFS wet up first, followed by SFS and HE. Assuming rain fell everywhere in the watershed, the offset of phase transition throughout the basin may be an indicator of differences in soil evaporation rates, where water input was evaporated prior to infiltration, versus transpiration which would likely have been at a minimum due to dormant vegetation. SFS likely had greater evaporative demand due to higher energy input from solar radiation and stored soil heat. The HE stations also transitioned later than NFS, but the driver(s) for higher evaporative demand were not clear and differences in the timing of wetting front infiltration may be attributable to differences in soil properties. Overall, the beginning of the fall wetting period occurred around the same time throughout the watershed, within a span of approximately ten days.

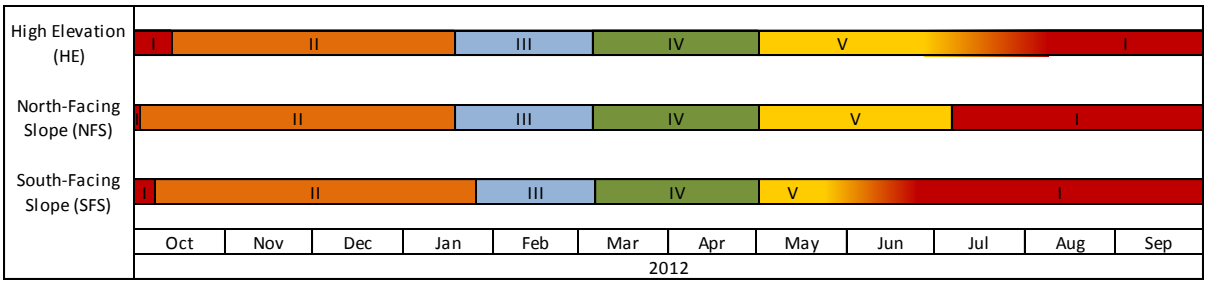

Figure 4-2. Timing of the five hydrologic seasons identified by McNamara et al. (2005) in the Johnston Draw watershed, 2012 water year: I) dry, II) transitional wetting, III) wet, low-flux, IV) wet, high-flux, V) transitional drying.

Phase III, as indicated by McNamara et al. (2005), was the winter wet, low flux period when streamflow initiated and stable soil moisture levels were near field capacity. McNamara et al. (2005) noted that upslope and downslope regions were hydraulically independent of each other during this period and vertical and lateral movement of soil moisture was limited. Should snow begin to accumulate prior to satisfying the soil moisture deficit, deeper soil zones would remain relatively dry throughout the winter months. This appeared to be the case at the HE sage and NFS locations between December and March. The soil temperatures were below freezing during these months and soil water content was unknown for these sites. Therefore, the behavior of the wetting front was indeterminable and the timing of transition from the fall wetting period to the winter wet, low-flux period (Phase III) can only be inferred based on precipitation inputs and snow cover. Based on that information, the transition to a winter wet, low-flux phase likely began with the mixed-precipitation event (Event 4) January 18, 2012 in the HE and NFS areas. Precipitation was stored as snow in these areas, greatly reducing water input to the soil. In contrast, the snowfall melted and infiltrated on the warmer SFS and was observed to increase soil moisture stored on that side of the drainage. The SFS transitioned to the winter wet, low-flux period one week later around January 25, 2012. Since the data were measured mid-slope in the drainage, there was no evidence whether upslope regions were disconnected hydraulically from downslope regions during this phase in Johnston Draw. What is evident in the data is that soil moisture on the SFS was near field capacity during the winter wet, low flux phase while NFS and HE soils likely remained dry at depth under an established snow cover. Additional winter precipitation and melt inputs on SFS were detectable as moderate flux near the surface (5 cm depth, Figure 3-1). It is difficult to compare the transitionally snow-covered SFS of Johnston Draw to Dry Creek because the study by McNamara et al. (2005) focused on a north-facing, snow dominated hill slope. Therefore,

the SFS in Johnston Draw may require a newly defined hydrologic season in which the soil moisture conditions are described as a hybrid between winter wet, low-flux and spring wet, high-flux periods.

Seasonal snow-melt marked the onset of the spring wet, high-flux phase (Phase IV) beginning March 5, 2012 at all locations in the drainage. Snow cover, where present, began to decline, soil moisture levels were near field capacity, and streamflow responded rapidly to water input. During the spring wet, high-flux phase, multiple snows were immediately followed by melt, producing multiple stream peaks and sustaining high seasonal flows. Towards the end of this hydrologic season, snowfall transitioned to mixed phase precipitation and rain. Although snow conditions differed between the different watershed regions, the concurrent shift between winter wet, low-flux and spring wet, high-flux periods suggests that warm seasonal temperatures and precipitation inputs were affecting hydrologic season change more than total snow depth or available soil water.

As air and soil temperatures warmed and vegetation began to transpire, evapotranspiration rates likely exceeded precipitation, marking the advent of the transitional late-spring drying period (Phase V). During this phase, soil water content and streamflow declined. Despite differences in elevation and aspect, the transitional drying phase began at approximately the same time at all locations in the watershed (May 1, 2012), similar to the synchronous transition of all locations to phase IV (wet, high-flux period). In both cases, the synchronous transition between hydrologic seasons correlated with large temperature changes despite differences in snow cover and soil conditions among opposing aspects. For example, the spring wet, high-flux period did not begin until air temperatures rose above 5°C even though snow cover on SFS had already been completely ablated. Towards the end of the spring wet, high-flux period, NFS stored more water and had cooler soil temperatures than SFS, yet the synchronous beginning of the transitional dry-down did not begin until minimum daily air temperatures rose above freezing and soil temperatures exceeded 5°C at 20 cm depth. Temporal synchronization of these hydrologic seasons across varying elevation and aspect indicate the strong influence of regional hydrometeorological seasonality over hydrologic phases and soil moisture states within the watershed. This seasonality apparently superseded the effect complex terrain may have had on hydrologic seasons during cooler months.

Significant differences in the timing of hydrologic seasons were observed during the warm months, where the transitional drying period (Phase V) was extended one to two months longer on NFS and HE. We infer that evapotranspiration exceeded precipitation during the warm season, based on declining soil moisture values, and the summer dry period (Phase I) began when moisture contents in the soil profile reached a minimum. During the summer dry period most precipitation was lost to evapotranspiration before the wetting front reached 20cm and the streambed was dry. High solar radiation inputs coupled with warm soil temperatures and limited water supply in the soil profile caused the SFS to enter this dry phase earlier than other parts of the watershed (Figure 4-1). Depending on the location, the soil moisture deficit reached maximum between the end of May and end of June on SFS. Deeper soils storing a larger water supply on NFS and at HE provided water for evaporation and transpiration later in the year and did not reach a maximum soil moisture deficit until the end of June to end of July. For the HE aspen location, the transitional drying phase extended into August before soils dried completely. These differences in soil water content between opposing aspects and higher elevations is most likely a function of soil depth rather than variances in precipitation phase or timing of snow melt. Deeper soils on NFS and at HE store more total water than SFS soils and are able to sustain transpiration in the warm season approximately one month longer, indicating that hydrologic seasons are somewhat controlled by soil properties.

The hydrologic seasons identified by McNamara et al. (2005) in Dry Creek correspond well with our observations of soil moisture conditions in Johnston Draw. In a later study of aspect effects on soil moisture storage and response, Geroy et al. (2011) found that NFS in Dry Creek stored more water than SFS and for longer into the summer season. They also noted that changes in soil wetting and drying were similar between opposing slopes. These findings are similar to observed soil moisture conditions on opposing aspects in Johnston Draw. The authors also noted that their manual measurements of soil moisture (0-15 cm depth) revealed greater volumetric water content on NFS than SFS. In contrast, our field measurements (0-30 cm depth) indicated that volumetric water content was relatively similar between NFS and SFS with the exception of the soils surrounding station 2b, which have been shown to have much higher clay content.

4.5 Streamflow Generation

The sources of streamflow generation in Johnston Draw can only be inferred, but data gathered for this analysis do provide for some insights into how this complex terrain is connected hydraulically to the stream channel. In evaluating streamflow generating events, rises in the hydrograph occurred during the cooler, typically wet months, when soil water content was at or near field capacity. Any water input from precipitation, snowmelt, or a combination of the two, corresponded with a nearly immediate hydrograph rise, typically 1-4 hours from the beginning of the event. The peaks fell off nearly as quickly once the rate of rain and/or snowmelt began to wane. This immediate response of the stream channel to storm and melt events indicates translatory flow mechanisms in the watershed, where pre-event stored water was likely displaced by new water during the event. No signs of overland flow in the watershed were observed during the two water years, despite several high-intensity rain-on-snow events and frozen soil conditions. The translatory flow mechanism was described as part of the variable source theory put forth by Hewlett and Hibbert (1967) and later observed in humid forest catchments (Pearce et al., 1986) and a semiarid forested region (Newman et al., 1998). Whether the translatory flow in Johnston Draw is via preferential flow pathways (i.e. macropores) or matrix flow is unknown, but the rapid response in streamflow to water input suggests that peak flows are comprised in large part by pre-event water stored in the basin.

Data from Johnston Draw also indicate that streamflow may be disproportionally supplied by different regions of the watershed, depending on the type of event and antecedent conditions. The NFS and HE regions stored more water than SFS in both the soil profile and in snowpack. While all regions of the watershed conceivably contributed water to runoff during storm events, NFS and HE areas may have contributed more water to stream runoff than SFS during specific types of events. If, for example, there was a rain-on-snow or melt event during those times that the NFS and HE had established snow cover and the SFS had little or no snow cover, the precipitation coupled with snowmelt would amount to a larger proportion of runoff volume from NFS and HE areas (e.g. Event 1, Event 5, Event 6). During other events, such as snow and mixed-phase precipitation events, where snow accumulated on NFS and HE, but was partly infiltrated on SFS and LE, resulting streamflow may have come disproportionally from SFS and LE (e.g. second half of

Event 2, Event 4). These types of events contributed to small rises in the hydrograph but were not typically the drivers for larger peaks in the flow record.

In the warm season, soils dried approximately one month earlier on SFS. During this offset of hydrologic seasons, where the NFS and HE were still in the transitional drying phase and the SFS were in the summer dry phase, stream flow volume was in decline and precipitation inputs did not wet below 20 cm depth. The bulk of streamflow during this period was most likely drainage from deep soil layers on the NFS and at HE. The stream channel completely dried around the same time that soil moisture storage reached minimum at these locations, indicating that the majority of flow from the end of June through August may have come from NFS and HE areas.

Chapter 5. Ecohydrological Implications

As the climate warms, efforts to project changes in hydrology, seasonality, and species occurrence are ongoing. Predicting the magnitude and spatial scale of these changes are underway through comprehensive modeling efforts and data collection campaigns in order that researchers and natural resource managers may plan for shifting ecohydrological landscapes. Globally, air temperatures are rising and the seasonal snowpack of mountainous regions is expected to decline in areal and temporal extent (e.g. Mote et al., 2005; Hamlet et al., 2007; IPCC, 2008; Nayak et al., 2010; Reba et al., 2011). Data records in snow dominated and transient snow watersheds indicate that warmer air temperatures are associated with decreased snow water equivalent, earlier snow melt, earlier spring peak flows and extended summer drought (Reba et al., 2011). Such shifts in seasonality and reduced available water during the growing season, coupled with increased evapotranspiration (Hamlet et al., 2007), will impact plant species composition in water stressed environments. Determining the spatial and temporal extent of species shifts, however, is limited by our understanding of sagebrush niches with respect to mass and energy balances in complex terrain. This discussion seeks to summarize some of the underlying assumptions made in predicting the effects of climate change on sagebrush ecosystems (*Artemisia* Spp.) and highlight how the analysis from Johnston Draw may contribute to defining ecohydrological niches and species distribution modeling efforts.

When referring to sagebrush ecosystems we are referring to the common sagebrush shrublands found in the western United Sates and characteristic of Johnston Draw, the location of our study. In addition to a range of sagebrush species, these shrublands encompass a variety of other shrubs and diverse perennial grasses (Bradley, 2010). Sagebrush ecosystems are used for grazing, recreation, and host a number of sagebrush obligate species such as *Cenrotcerus urophasianus* (greater sage-grouse) and *Brachylagus idahoensis* (pygmy rabbit) (Bradley, 2010; Schlaepfer et al., 2012). Land management, invasive species, and global climate change threaten sagebrush ecosystems and hence, vulnerable obligate species (Bradley, 2010). As natural resource managers are faced with the challenge of planning for projected future climate conditions, improved species habitat models are needed to inform conservation decisions.

Very little work has been done to determine the effects of a warming climate on sagebrush habitat. In a Colorado montane meadow, vegetation plots hosting big sagebrush (*Artemisia*

Tridentata) were manually warmed by applying overhead infrared radiation and heated 3-6°C above the daytime temperatures of control plots (Perfors et al., 2003). The effects of this manual warming resulted in slightly warmer soils (approximately 1.5°C increase in the upper 15 cm), shorter duration snow pack (melted 20 days prior to control), and drier soils (15% less gravimetric water content). Unfortunately there was no context for the topography of the study site and therefore, we must assume that the area was relatively low gradient with little topographical influence. Bradley (2010) used empirical models to determine risk to sagebrush ecosystems in Nevada and found that areas of high risk from climate change were in the southern and western parts of the state. While the methods of this study were well documented, the assumptions made to determine climatic constraints on sagebrush habitat were not clearly stated. Apparently the assessment of suitable sagebrush habitat hinged on comparisons of average monthly and annual precipitation, minimum temperature, and maximum temperature. Elevation was certainly considered, but there was no mention of slope aspect, steepness, precipitation regime, or soil characteristics. Another modeling exercise conducted in eastern Idaho used historical climate and species occurrence data to identify key parameters to survival and growth of *Artemisia tripartita* (three-tipped sagebrush) for understanding future climate effects (Dalgleish et al., 2011). They found that larger individuals had better survival rates and also that higher snowfall in February and March increased recruitment of *A. tripartita*, most likely due to increased availability of soil water in the spring. Site topography and soils were neither defined nor considered in the analysis of this sagebrush ecosystem. For both the Nevada and Idaho studies, defining sagebrush habitat focused on correlating easily obtained climate indicators such as precipitation and temperature with species occurrence and survival rates. Within these empirical relationships, the influence of temperature and precipitation on soil water dynamics was inferred, but not directly addressed by any of the habitat models. Therefore, much of the underlying water balance processes affecting sagebrush habitat remains unknown in these ecosystem models.

Another approach to forecasting the effects of climate change on species is to use species distribution modeling, or SDM. Conventionally, SDMs have correlated species occurrence data with environmental data to extrapolate a climatic niche for species distribution. SDMs are not universally accepted however, and have been criticized for developing correlational relationships beyond observed data (Schlaepfer et al., 2011). This is due in part to the fact that SDMs are based on ecosystem niche models, which incorporate such a vast array of variables that some

assumptions must be made, and also to the uncertainties introduced by climate projections based on different general circulation models (Wiens et al., 2009). To improve SDM in sagebrush ecosystems, Schlaepfer et al. (2011) compared conventional climate-based SDM with a process-based approach using simulations of water balance. The study covered big sagebrush (*A. tridentata*) dominated ecosystems throughout the western United States. Overall, the SDM predicted decreases in species occurrence for southern latitudes and lower elevations and increased species occurrence for northern latitudes and higher elevations. Comparison of the different datasets used in the SDM indicated that minimum air temperature and precipitation regime were important factors in determining the presence and shift of sagebrush ecosystems. As with other modeling studies, a discussion of the explicit assumptions made during the modeling process was lacking. Generally, the restriction of pixel size from regional Gap Analysis Program data (900 m^2), and the re-projecting of all spatial data to an equal area grid of 100 km^2, indicated the scale of homogeneity assumed in the analysis. The method of applying equal area projection to the SDM incorporated a large amount of uncertainty when considering the evidence that water balance estimates have been shown to be sensitive to topographic variations at scales of less than 1 km^2 (Chauvin et al., 2011). The authors do note these limitations in the discussion of their results. Hydrometeorological point data, such as that produced by our study, can be used to improve process-based SDM modeling by quantifying the relatively small scale variations of hydrometeorological conditions that occur within complex terrain.

The dataset from our study will also assist in defining the niche of sagebrush ecosystems as it is one of the most detailed datasets on snow and soil variations in complex terrain spanning the critical rain-snow elevation band. When discussing species aggregation and patchiness, spatial scale may be based on both elevation and aspect. Information from our study can help extrapolate site characteristics and ecological niches for modeling spatial and temporal changes in ecosystem distributions. As with SDM, conventional species niche definition has been based primarily on climatic, latitudinal, and elevation constraints. In an effort to improve predictions for sagebrush ecosystems, Schlaepfer et al. (2012) endeavored to define an ecohydrological niche for sagebrush ecosystems based on integrated climate and soil water controls. The study modeled different sagebrush ecosystem types using SOILWAT to simulate water balance in space and time for sites across the western United States. From this exercise, three ecological niches were identified, partitioned by several parameters including elevation, general soil characteristics and mean annual temperatures and precipitation. Overall, the ecohydrological niche of sagebrush ecosystems was

characterized by spring recharge to soil water followed by a summer dry period where top soil layers dried earlier than bottom soil layers. Naturally, soil depth was observed to be an important determinant of the water balance in SOILWAT simulations. And soil depth, in addition to several other defining attributes of sagebrush ecosystems were used to define the spatial extent of three sagebrush ecosystems at a very coarse scale that covered 3.1×10^6 km^2 across 11 western states. The dataset produced by our study illustrates that many of the factors used to define these ecohydrological niches (e.g. soil water, soil temperature, timing of soil dry down) vary considerably at the same elevation on opposing aspects. Combined with finer scale species occurrence data, information from our study can be used to refine the scale at which ecohydrological niches are defined. This would, in turn, translate into greater resolution of SDMs and assessments of risk to sagebrush ecosystems, especially in areas along the rain-snow transition zone where rapid transitions are expected to occur.

Overall, recent efforts to forecast climate change effects on sagebrush ecosystems have involved using remotely sensed data at coarser scales (900 m^2 to 100 km^2) and generalized climate indicators such as mean annual temperature, mean annual precipitation, and air temperature minimums and maximums. The outputs of these niche and species distribution models are constrained spatially by latitude and elevation. Other features of complex topography such as aspect and slope have yet to be considered despite the evidence that these factors influence soil water dynamics (Chauvin et al., 2011; Geroy et al., 2011) and species occurrence (Bales et al., 2006). A challenge for improving models of species niche and distribution is in meshing multiple scales of data. Datasets such as ours are based on point measurements arranged at scales of 10 m to 2 km. The spatial and temporal scale of our study is limited and would need to be combined with similar measurements in catchments across the western United States to realistically project the effects of complex terrain on species niche and distribution. Meshing data from point measurements with remote sensing information is proving to be a difficult challenge, but one that must be met if we are to improve resolution and decrease uncertainty in our models (Seyfried and Wilcox, 1995; Bales et al., 2006; Wiens et al., 2009).

Based on the results of our study and the literature examining potential effects of climate change on sagebrush ecosystems, we can speculate on what the future may hold for vegetation assemblages in Johnston Draw. Increases in air temperature will certainly increase evaporation and transpiration demand. With shallower soils and less available water on SFS than NFS, the water

limitation will likely reduce sagebrush viability and recruitment potential on SFS and increase favorable conditions on NFS. As temperatures increase, the snow dominated NFS and upper elevations of the watershed will likely transition to snow dynamics similar to those currently observed on SFS. Where once snow cover persisted for months, the cover will begin to melt earlier and eventually winter snow events will melt more frequently throughout the winter lasting only days to weeks. Eventually, if temperatures continue to rise, the rain-snow transition elevation will migrate above the top of the watershed and Johnston Draw will be completely rain-dominated. Our examination of the coupling of snow cover, soil temperature, and soil moisture in Johnston Draw indicated that precipitation phase had little effect on the timing of soil dry down. Despite differences in soil moisture infiltration on opposing aspects, the onset of soil dry down began simultaneously throughout the watershed when seasonal shifts in air and soil temperature began. Therefore, it is reasonable to assume that changes in precipitation phase alone will not drastically affect sagebrush occurrence in Johnston Draw. Rather, greater influence may come from the shifting of seasons to earlier in the year. Such changes could prove to be advantageous for annual forbs and grasses at the expense of perennial species. Lastly, soil temperatures in Johnston Draw may become more variable with the warming climate, including higher maximums in the summer months and lower minimums in the winter months associated with the loss of insulating snow cover. Freezing soil temperatures and exposed soils in the winter could adversely impact winter survival rates of sagebrush species. Coupling our data with the results of modeling efforts to predict shifts in sagebrush ecosystem occurrence, we would expect to see reduced species occurrence at the lower elevations on SFS that gradually shifts upwards in elevation, and possibly some reduction at the lower elevations of the NFS. Upper elevations of the SFS and mid- and upper elevations of NFS will likely support sagebrush ecosystems longer into the next century despite projected changes in precipitation phase.

To date, the majority of research concerning climate change impacts on sagebrush ecosystems has been primarily based on empirical modeling and the correlation of easily measured climate variables with species occurrence data. In addition, the scope of these studies have been broad in scale, using remote sensing data (finest resolution 30 m x 30 m), and spanning hundreds of thousands of square kilometers. One exception is the study by Dalgleish et al. (2011) that correlated climate data with species demography within 1 m^2 plots. Another exception is the work advanced by Schlaepfer et al. (2011 and 2012) that incorporated soil water balance into species niche and distribution modeling. While these extrapolative large-scale studies are useful for land

and resource management, there remains the pressing need to better understand the relationships between species and environment through a more mechanistic approach. What are the processes through which hydrometeorological conditions, complex terrain, and species physiology are coupled? At what spatial scale does the interaction of soil water dynamics with species occurrence become relevant? How resilient are sagebrush ecosystems to changes in snow accumulation and earlier melt rates? And perhaps most importantly, how do we mesh the scales of these mechanistic processes with remote sensing and regional datasets? As these and similar questions are explored, complex topography should be considered when determining relationships between biological and environmental data, whether they are correlational or mechanistic. The results of our study indicate that complex terrain plays an important role in the spatial variability of snow dynamics, soil moisture, and soil temperature and quantifies those differences over spatial scales of less than 1 km distance and 100 m elevation change. Therefore it is reasonable to assume that topography influences the ecohydrologic niche and dynamics of sagebrush ecosystems as well.

Chapter 6. Conclusions

Quantifiable differences in snow cover, soil moisture, and soil temperature throughout the watershed, particularly on opposing slopes, demonstrate how these hydrometeorological variables are coupled in complex terrain. Snow cover on SFS was observed to be transient in nature, lasting only days to weeks and accumulating approximately one-half the depth of the seasonally persistent snow pack on NFS. While our data do not demonstrate causality, differences in snow dynamics between opposing slopes are likely linked to differences in energy inputs from solar radiation and stored soil heat. Soil temperatures in the watershed were consistently warmer on SFS and experienced greater diurnal fluctuation than NFS, with average annual temperatures ranging between 5 °C and 6 °C higher year round at depths of 50 cm or less. This difference in soil temperatures, observed at the same elevation on opposing aspects, was similar in magnitude to the soil temperature differences observed at low-relief stations 900 m elevation apart in the Reynolds Creek Experimental Watershed. The coupling of snow dynamics with soil temperature and soil moisture result in two distinct snow seasons and growing seasons at similar elevations in the watershed.

Observed soil moisture states in Johnston Draw corresponded well with the five hydrologic seasons identified by McNamara et al. (2005), however some distinct differences were noted in the larger, more complex Johnston Draw watershed. The most notable difference was during the transitional drying phase when NFS and HE areas continued to provide water approximately one month longer than the SFS. Our data do not indicate the cause of this discrepancy, but there is a correlation between soil depth and the total amount of water stored in the soil, which would explain why the shallower SFS dried out much earlier than other areas of the watershed. Less obvious, but also quite noteworthy, was that the other hydrologic seasons were synchronized at different elevations and across opposing aspects. This was anticipated for the summer dry, winter wet low-flux, and spring wet high-flux periods. However, SFS were expected to begin drying down much earlier than NFS due to warmer soil temperatures and higher shortwave radiation. Instead, data for both water years indicated that the onset of the spring transitional drying period was simultaneous throughout the watershed. This evidence suggests that the transitional drying phase in this rain-snow transition zone is independent of the complex terrain and more heavily influenced by seasonal fluctuations in temperature and solar radiation. With continued climate warming,

hydrologic seasonality may change from a five phase system to a four phase system as seasonal snow melt declines, effecting the spring wet, high flux period. This would likely result in earlier streamflow peaks that were attenuated in volume and extended temporally. Other hydrologic seasons (and corresponding runoff generation) may be less impacted by temperature increases and more dependent on precipitation changes such as the fall transitional wetting and winter wet, low-flux periods.

An examination of hydrometeorological variables coupled with streamflow revealed that runoff generating events occurred primarily between late-fall and spring, corresponding with mixed-phase precipitation, rain-on-snow, midwinter melt, and seasonal melt events. Only one rain event was correlated with significant (>2cm) increase in stream stage, occurring in the spring of 2012, when soils were near field capacity. Streamflow response to water input during these events was almost immediate, with delays between 1-4 hours. Such short time lags between the precipitation or melt event and changes in stream stage suggest that translatory flow mechanisms are present in the watershed, although this assertion is speculative and more detailed study is needed. A closer inspection of the antecedent conditions coupled with water inputting events reveal scenarios in which streamflow may consist of disproportionate runoff from various regions of the watershed. Examples of this include rain-on-snow events, where snow cover is present on NFS and HE and ablated on SFS and LE. The water inputs from rain and snowmelt combined in the NFS and HE are likely much greater than those from SFS and LE areas with no snow and limited soil water storage capacity. When mixed-phase events result in snow accumulation on NFS and HE areas and water infiltration on bare SFS and LE areas, then the reverse is likely where the larger proportion of runoff is contributed by SFS and LE regions of the watershed. Our analysis reveals the complex flow generation patterns and processes in complex terrain spanning the rain-snow transition zone.

Finally, the results of this study were incorporated with a literature review of expected effects of climate warming on sagebrush ecosystems. Few studies to date address this question and the majority of those that were examined involved empirical modeling using remote sensing data and covering large regions (>100-10,000 km^2). In contrast, our detailed dataset spanned a single watershed (approximately 2 km^2) and would be better suited to a process-based approach where the coupling of complex terrain, hydrometeorological variables, and sagebrush physiology are examined and scaled up to the surrounding region. A conceptual model of the effects of

climate warming on sagebrush ecosystems in Johnston Draw was developed by integrating the results of this study with those from the reviewed research. As air temperatures rise and precipitation transitions from rain to snow, sagebrush and obligate species will likely decline at the lower elevations of the watershed and on SFS and increase at higher elevations and on NFS. Future conditions on NFS may be very similar to current conditions on SFS in terms of snow dynamics and species assemblages. The model put forth from this analysis is speculative and additional study would be required to determine the likelihood of such changes in response to expected climate warming.

The detailed hydrometeorological dataset produced by this study indicate the importance of considering complex terrain in our efforts to better understand interactions between hydrologic patterns and processes. Traditionally, hydrologic datasets have been dominated by measurements from snow-dominated or low relief areas. Those regions characterized by high-relief and variable aspects within the rain-snow transition zone are underrepresented in the data record. Continued monitoring and strategically placed measurements are needed to fill the knowledge gap and support research on runoff processes and ecohydrology in semi-arid mid-latitude regions.

References

Bales, R.C., Hopmans, J.W., O'Geen, A.T., Meadows, M., Hartsough, P.C., Kirchner, P., Hunsaker, C.T., and Beaudette, D., 2011, Soil Moisture Response to Snowmelt and Rainfall in a Sierra Nevada Mixed-Conifer Forest: Vadose Zone Journal, v. 10, no. 3, p. 786, doi: 10.2136/vzj2011.0001.

Bales, R.C., Molotch, N.P., Painter, T.H., Dettinger, M.D., Rice, R., and Dozier, J., 2006, Mountain hydrology of the western United States: Water Resources Research, v. 42, no. 8, p. 1–13, doi: 10.1029/2005WR004387.

Bradley, B. a., 2010, Assessing ecosystem threats from global and regional change: hierarchical modeling of risk to sagebrush ecosystems from climate change, land use and invasive species in Nevada, USA: Ecography, v. 33, no. 1, p. 198–208, doi: 10.1111/j.1600-0587.2009.05684.x.

Broxton, P.D., Troch, P. a., and Lyon, S.W., 2009, On the role of aspect to quantify water transit times in small mountainous catchments: Water Resources Research, v. 45, no. 8, p. n/a–n/a, doi: 10.1029/2008WR007438.

Chauvin, G.M., Flerchinger, G.N., Link, T.E., Marks, D., Winstral, a. H., and Seyfried, M.S., 2011, Long-term water balance and conceptual model of a semi-arid mountainous catchment: Journal of Hydrology, v. 400, no. 1-2, p. 133–143, doi: 10.1016/j.jhydrol.2011.01.031.

Dalgleish, H.J.., Koons, D.N., Hooten, M.B., Moffet, C.A., and Adler, P.B., 2011, Climate influences the demography of three dominant sagebrush steppe plants: Ecology, v. 92, no. 1, p. 75–85.

Ebel, B. a., 2012, Impacts of Wildfire and Slope Aspect on Soil Temperature in a Mountainous Environment: Vadose Zone Journal, v. 11, no. 3, doi: 10.2136/vzj2012.0017.

Gee, G.W., and Bauder, J.W., 1986, Hydrometer Method, *in* Klute, A. ed., Methods of Soil Analysis, Part 1, American Society of Agronomy, Inc., Soil Science Society of America, Inc., Madison, WI, p. 404–411.

Geroy, I.J., Gribb, M.M., Marshall, H.P., Chandler, D.G., Benner, S.G., and McNamara, J.P., 2011, Aspect influences on soil water retention and storage: Hydrological Processes, v. 25, no. 25, p. 3836–3842, doi: 10.1002/hyp.8281.

Grant, L., Seyfried, M., and McNamara, J., 2004, Spatial variation and temporal stability of soil water in a snow-dominated, mountain catchment: Hydrological Processes, v. 18, no. 18, p. 3493–3511, doi: 10.1002/hyp.5798.

Hamlet, A.F., Mote, P.W., Clark, M.P., and Lettenmaier, D.P., 2007, Twentieth-Century Trends in Runoff, Evapotranspiration, and Soil Moisture in the Western United States*: Journal of Climate, v. 20, no. 8, p. 1468–1486, doi: 10.1175/JCLI4051.1.

Hewlett, John D and Hibbert, A.R., 1967, Factors affecting the response of small watersheds to preciptiation in humid areas, in Sopper, W.E. and Lull, H.W. eds., International Symposium on Forest Hydrology, Pergamon, New York, p. 275–290.

IPCC, 2008, Observed and projected changes in climate as they relate to water, *in* Bates, B.C., Kundzewicz, Z.W., Wu, S., and Palutikof, J.P. eds., Climate Change and Water, IPCC Technical Paper VI-June, IPCC Secretariat, Geneva, p. 210.

Jones, S.B., Wraith, J.M., and Or, D., 2002, Time domain reflectometry measurement principles and applications: Hydrological Processes, v. 16, no. 1, p. 141–153, doi: 10.1002/hyp.513.

Kang, S., Kim, S., Oh, S., and Lee, D., 2000, Predicting spatial and temporal patterns of soil temperature based on topography, surface cover and air temperature: Forest Ecology and Management, v. 136, no. 1-3, p. 173–184, doi: 10.1016/S0378-1127(99)00290-X.

Lyon, S.W., Troch, P.A., Broxton, P.D., Molotch, N.P., and Brooks, P.D., 2008, Monitoring the timing of snowmelt and the initiation of streamflow using a distributed network of temperature / light sensors: Ecohydrology, v. 224, no. 1, p. 215–224, doi: 10.1002/eco.

Marks, D., Winstral, A., Reba, M., Pomeroy, J., and Kumar, M., 2012, An Evaluation of Methods for Determining During-Storm Precipitation Phase and the Rain/Snow Transition Elevation at the Surface in a Mountain Basin: Advances in Water Resources, v. online art, doi: 10.1016/j.advwatres.2012.11.012.

McNamara, J.P., Chandler, D., Seyfried, M., and Achet, S., 2005, Soil moisture states, lateral flow, and streamflow generation in a semi-arid, snowmelt-driven catchment: Hydrological Processes, v. 19, no. 20, p. 4023–4038, doi: 10.1002/hyp.5869.

Mote, P.W., Hamlet, A.F., Clark, M.P., and Lettenmaier, D.P., 2005, Declining Mountain Snowpack in Western North America*: Bulletin of the American Meteorological Society, v. 86, no. 1, p. 39–49, doi: 10.1175/BAMS-86-1-39.

Nayak, A., Marks, D., Chandler, D.G., and Seyfried, M., 2010, Long-term snow, climate, and streamflow trends at the Reynolds Creek Experimental Watershed, Owyhee Mountains, Idaho, United States: Water Resources Research, v. 46, no. 6, p. 1–15, doi: 10.1029/2008WR007525.

Newman, B.D., Campbell, A.R., and Wilcox, B.P., 1998, Lateral subsurface flow pathways in a semiarid Ponderosa pine hillslope: Water Resources Research, v. 34, no. 12, p. 3485, doi: 10.1029/98WR02684.

Newman, B.D., Wilcox, B.P., and Graham, R.C., 2004, Snowmelt-driven macropore flow and soil saturation in a semiarid forest: Hydrological Processes, v. 18, no. 5, p. 1035–1042, doi: 10.1002/hyp.5521.

Pearce, A.J., Stewart, M.K., and Sklash, M.G., 1986, Pearce 1986.pdf: Water Resources Research, v. 22, no. 8, p. 1263–1272.

Perfors, T., Harte, J., and Alter, S.E., 2003, Enhanced growth of sagebrush (Artemisia tridentata) in response to manipulated ecosystem warming: Global Change Biology, v. 9, p. 736–742.

Pierson, F.B., Slaughter, C.W., and Cram, Z.K., 2001, Long-Term Stream Discharge and Suspended-Sediment Database, Reynolds Creek Experimental Watershed, Idaho, United States: Water Resources Research, v. 37, no. 11, p. 2857, doi: 10.1029/2001WR000420.

Reba, M.L., Marks, D., Winstral, A., Link, T.E., and Kumar, M., 2011, Sensitivity of the snowcover energetics in a mountain basin to variations in climate: Hydrological Processes,, p. n/a–n/a, doi: 10.1002/hyp.8155.

Schlaepfer, D.R., Lauenroth, W.K., and Bradford, J.B., 2012, Ecohydrological niche of sagebrush ecosystems: Ecohydrology, , no. 5, p. 453–466, doi: 10.1002/eco.238.

Schlaepfer, D.R., Lauenroth, W.K., and Bradford, J.B., 2011, Effects of ecohydrological variables on current and future ranges , local suitability patterns , and model accuracy in big sagebrush: Ecography, , no. 000, p. 1–11, doi: 10.1111/j.1600-0587.2011.06928.x.

Seyfried, M.S., and Wilcox, B.P., 1995, Scale and the nature of spatial variability: Field examples having implications for hydrologic modeling: Water Resources Research, v. 31, no. No. 1, p. 173–184.

Stevens Water Monitoring Systems Inc., 2007, Comprehensive Stevens Hydra Probe Users Manual 92915:, 1–63 p.

Wiens, J.A., Stralberg, D., Jongsomjit, D., Howell, C.A., and Snyder, M.A., 2009, Niches , models , and climate change : Assessing the assumptions and uncertainties: PNAS, v. 106, p. 19729–19736.

Wilcox, B.P., Newman, B.D., Brandes, D., Davenport, D.W., and Reid, K., 1997, Runoff from a semiarid ponderosa pine hillslope in New Mexico: Water Resources Research, v. 33, no. 10, p. 2301–2314.

Williams, C.J., Mcnamara, J.P., and Chandler, D.G., 2009, Controls on the temporal and spatial variability of soil moisture in a mountainous landscape : the signature of snow and complex terrain: Hydrology and Earth System Sciences, , no. 13, p. 1325–1336.

Winstral, A., and Marks, D., 2002, Simulating wind fields and snow redistribution using terrain-based parameters to model snow accumulation and melt over a semi-arid mountain catchment: Hydrological Processes, v. 16, no. 18, p. 3585–3603, doi: 10.1002/hyp.1238.

Winstral, A., Marks, D., and Gurney, R., 2013, Simulating wind-affected snow accumulations at catchment to basin scales: Advances in Water Resources, v. 55, p. 64–79, doi: 10.1016/j.advwatres.2012.08.011.

Appendix A. Soil Characteristics

The following data summarize layer and soil characteristics from four soil pits dug near Johnston Draw automated stations 2, 4, 2b, and 4b (Tables A-1 through A-4). Those layers within identified B/C horizons were further analyzed for particle size distribution in the clay and silt fraction (Figure A-1). Percentage of gravel, sand, silt, and clay were determined for each layer tested, and a weighted average for the B and C horizons of the pedon determined (Table A-5).

Table A-1. Soil characteristics observed near Station 2b.

Station 2b
Soil Pit Location: 0517677, 4774808 (UTM11, 5m acc.)

Hzn	Layer #	Depth (cm)	Hzn Transition	% Rocky Fragments	Roots	Structure			Rupture Resistance		Color		Sedimentation Analysis			
						Type	Size	Grade	Moist	Dry	Moist	Dry	% Gravel	% Sand	% Silt	% Clay
Oi	1	0-1		<15												
A	2	1-3	abrupt, smooth	<15	very fine, few	granular	medium	strong		moderately hard	5YR 3/2	5YR 4/2				
B1	3	3-13	very abrupt, smooth	<15	fine, common	angular blocky	fine medium	strong	very firm	hard	5YR 3/2	5YR 4/4	23.2	44.7	19.0	13.0
B2	4	13-20	clear, smooth	15 to <35	fine, common	angular blocky	coarse	strong	slightly rigid	moderately hard	5YR 2.5/2 7.5YR 3/4	5YR 4/2 7.5YR 4/4	23.2	41.6	19.8	15.4
B/Cr1	5	20-50	abrupt, wavy	15 to <35	fine, common	angular blocky	very coarse	strong	slightly rigid	hard	7.5YR 4/6	7.5YR 5/6	21.8	41.7	16.7	19.7
B/Cr2	6	50-75	clear, wavy	<15	fine, common	angular blocky / platy	coarse medium / coarse	strong / strong		hard	7.5YR 5/8	7.5YR 6/8	14.6	47.6	18.6	19.2

Notes: Encountered soil moisture increase in layer 5. Soil cemented and very difficult to excavate below 3 cm depth with increasing difficulty corresponding to depth.

Table A-2. Soil characteristics observed near Station 4b.

Station 4b
Soil Pit Location: 517238, 4774859 (UTM11, 5m acc.)

Hzn	Layer #	Depth (cm)	Hzn Transition	% Rocky Fragments	Roots	Structure			Cementation Class	Rupture Resistance (Dry)	Color		Sedimentation Analysis			
						Type	Size	Grade			Moist	Dry	% Gravel	% Sand	% Silt	% Clay
Oi	1	0-2														
A	2	2-16	abrupt, smooth	<15	very fine/fine common/many	granular	medium	strong	friable	slightly hard	7.5YR 2.5/2	5YR 4/2	16.9	44.7	19	13.1
B	3	16-20	very abrupt, wavy	45	fine, many	angular blocky	very fine	strong	very firm	moderately hard	5YR 2.5/2	7.5YR 4/2	21.2	41.6	19.8	15.4
Cr1	4	20-28	abrupt wavy	45	med-coarse, common	angular blocky	medium-coarse	strong	extra firm	very hard	7.5YR 2.5/3	7.5YR 4/3	17.9	41.7	16.7	19.7
Cr2	5	28-35	clear wavy	65	medium, common	angular blocky	coarse	strong	extra firm	very hard	7.5YR 2.5/3	7.5YR 4/3	21.8	47.6	18.6	19.2
R	6	>35	abrupt wavy	boulders												

Notes: macropores observed in upper 20 cm consisting of tubular 2-5mm; rocky fragments primarily fine gravel and medium to fine gravel in Cr layers 4 & 5.

Table A-3. Soil characteristics observed near Station 2.

Station 2																
						Structure					Color		Sedimentation Analysis			
Hzn	Layer #	Depth (cm)	Hzn Transition	% Rocky Fragments	Roots	Type	Size	Grade	Cementation Class	Rupture Resistance (Dry)	Moist	Dry	% Gravel	% Sand	% Silt	% Clay
Oi	1	0-2														
A	2	2-9	clear, wavy		very fine, many; fine&med, common; coarse, few	sub-angular blocky	fine	weak	friable	slightly hard	5YR 2.5/2	7.5YR 5/2	13	67.7	17.2	2.2
Bw1	3	9-25	gradual, wavy	gravelly	very fine & fine, common; med, few	sub-angular blocky	fine	weak	firm	slightly hard	7.5YR 2.5/2	7.5YR 4/2	12.9	56.2	27.0	3.9
Bw2	4	25-47	diffuse, irregular	gravelly	very fine-med common; coarse, v.few	columnar / sub-angular blocky	fine / med & fine	weak	firm	moderately hard	7.5YR 2.5/3	7.5YR 4/3	22.2	57.8	17.5	2.5
Bw3	5	47-60	diffuse, wavy	very gravelly	very fine & fine, common; med, few	angular blocky	fine	weak	firm	moderately hard	7.5YR 3/3	10YR 4/3	28.8	21.0	16.2	3.9
B	6	60-70	diffuse, wavy	extremely gravelly	med, few; very fine, common	angular blocky	med & fine	moderate	firm	moderately hard	7.5 YR 4/4	10YR 6/4	35.1	45.4	16.7	2.8
Notes: rock fragments increase with depth																

Table A-4. Soil characteristics observed near Station 4.

Station 4																
						Structure					Color		Sedimentation Analysis			
Hzn	Layer #	Depth (cm)	Hzn Transition	% Rocky Fragments	Roots	Type	Size	Grade	Cementation Class	Rupture Resistance (Dry)	Moist	Dry	% Gravel	% Sand	% Silt	% Clay
Oi	1	0-3														
A	2	3-8	abrupt, smooth	none	very fine-med, common	sub-angular blocky	fine	moderate	friable	slightly hard	10YR 2/2	10YR 3/3				
Bw1	3	8-33	gradual, smooth	none	very fine-med, common; coarse, few	angular blocky	med & fine	moderate	friable	slightly hard	10YR 2/2	10YR 3/4	12.4	71.0	15.5	1.1
Bw2	4	33-62	diffuse, smooth	none	very fine-med, common; coarse, very few	sub-angular blocky	fine	moderate	friable	slightly hard	10YR 2/2	10YR 3/3	7.0	76.5	16.5	0.0
B	5	62-75	diffuse, smooth	med gravel <10	very fine-med, common; coarse, very few	angular blocky	medium	moderate	firm	moderately hard	7.5YR 4/2	7.5 YR 2.5/2	9.3	69.8	20.6	0.2
Notes: rock fragments increase with depth																

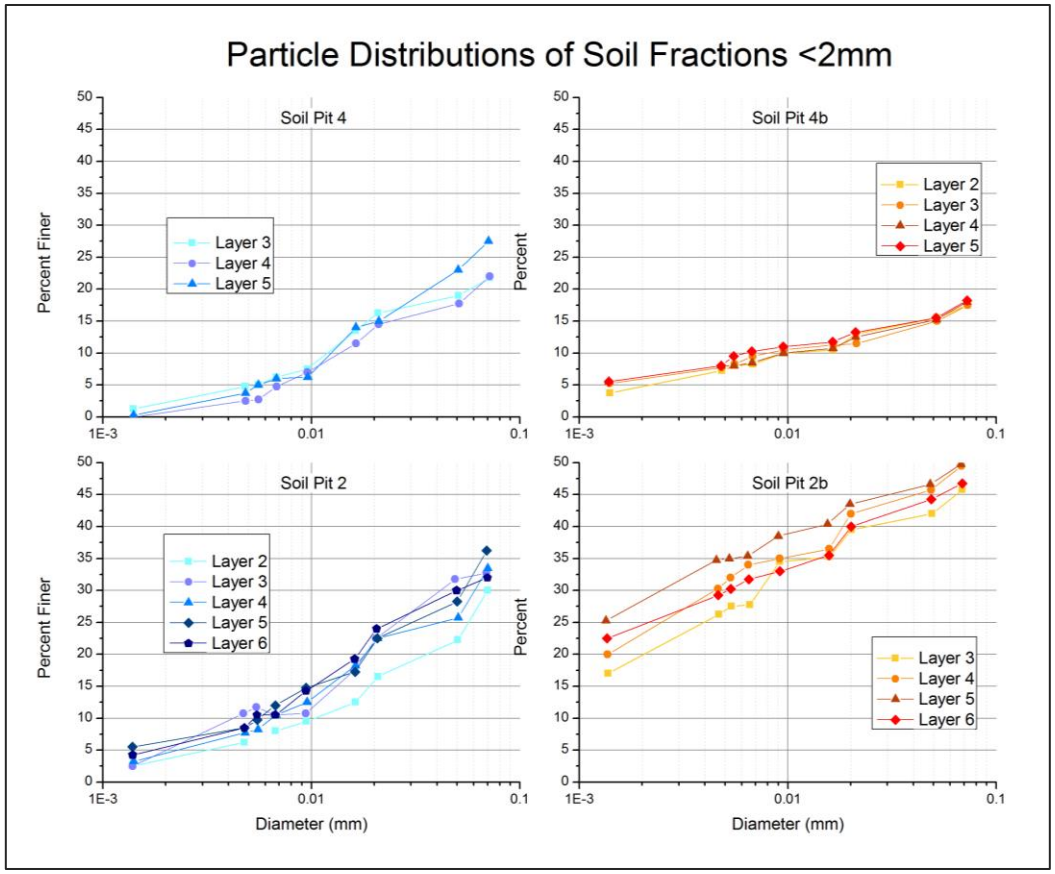

Figure A-1. Particle size distributions of the soil fraction less than 2mm in diameter for each layer/soil pit. Particle diameter and percentages determined with hydrometer method (Gee & Bauder, 1986).

Table A-5. Weighted pedon average, fine earth fraction, and soil texture class in the B/C horizons of sampled soils.

Soil Pit	Weighted Average % Clay	Weighted Average % Silt	Weighted Average % Sand	Weighted Average % Gravel
2b	18.2	18.0	44.2	19.6
4b	3.8	8.7	68.8	18.7
2	3.1	19.3	55.3	22.2
4	0.5	17.0	73.1	9.5
Soil Pit	**Fine Earth % Clay**	**Fine Earth % Silt**	**Fine Earth % Sand**	**Texture Class**
2b	22.6	22.4	55	Gravelly sandy clay loam
4b	5.7	10.7	84.6	Gravelly loamy sand
2	4	24.7	71.2	Gravelly sandy loam
4	0.5	18.7	80.8	Loamy sand

Appendix B. Meteorological Data for Water Years 2011 and 2012

The following figures contain data from automated meteorological stations in Johnston Draw between January 1, 2011 and October 1, 2012, measured in 15 minute increments. Where averages are presented, data for each time increment is the mean of multiple measurement locations. The solar radiation data are averaged measurements from stations 124 and 125. Wind Speeds are averaged by watershed region, where station 124 represents the ridge area, stations 2b, 3b, 4b, and 124b are averaged together to represent the south-facing slope, station 3 represents the north-facing slope, and station 125 is the low elevation location. Air temperature, vapor pressure, and dew point temperature data are the mean of all automated meteorological stations: 124, 124b, 125, 1, 2, 3, 4, 5, 2b, 3b, and 4b. Cumulative precipitation is the sum of precipitation measured by shielded Belfort Gauge every 15 minutes at stations 124, 124b, and 125. Snow depth data are displayed in 15 minute increments for each individual station.

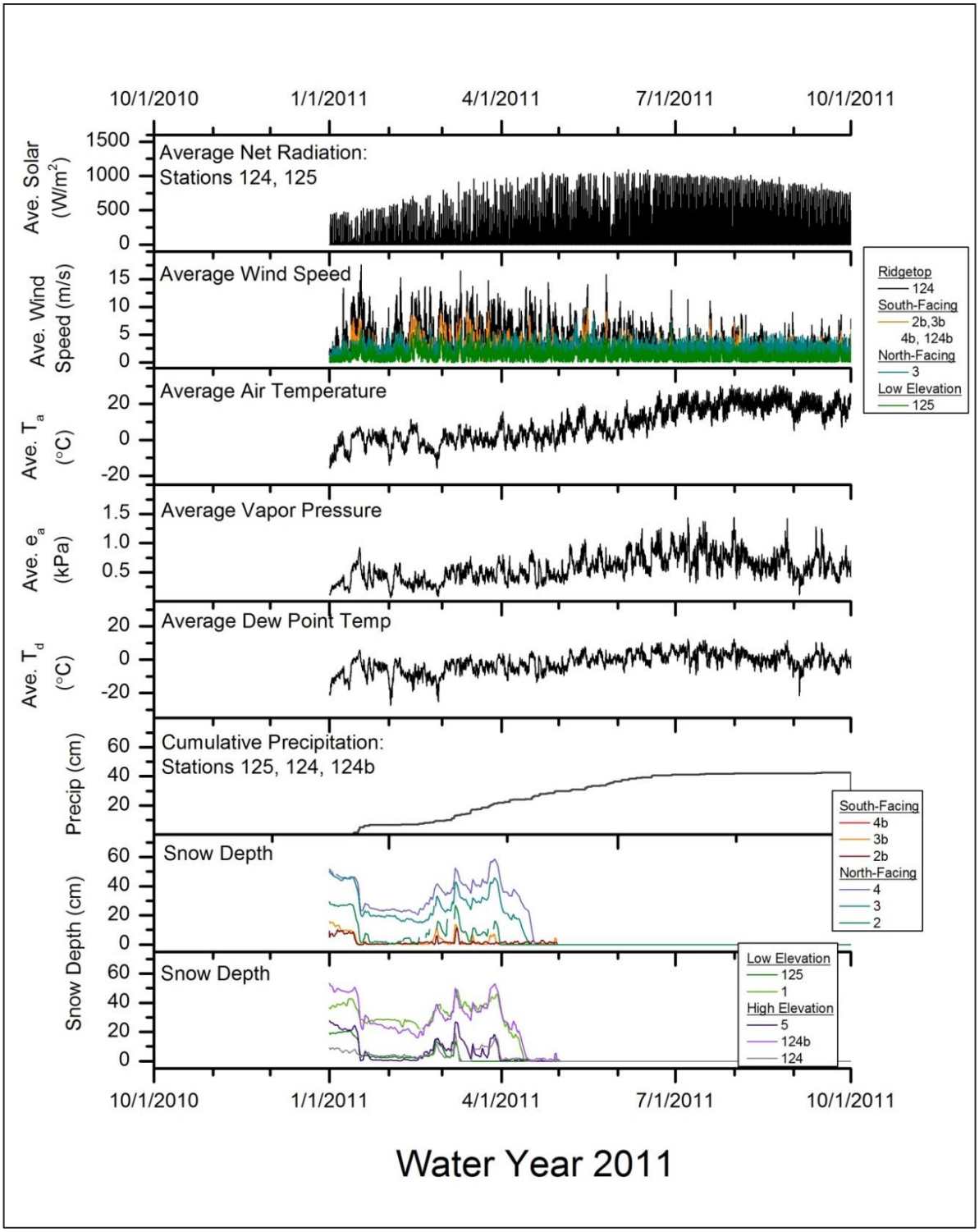

Figure B-1. Meteorological data for water year 2011 in Johnston Draw. The term "average" refers to spatial averages, rather than temporal, and includes all meteorological stations except where noted: net radiation, wind speed, and snow depth.

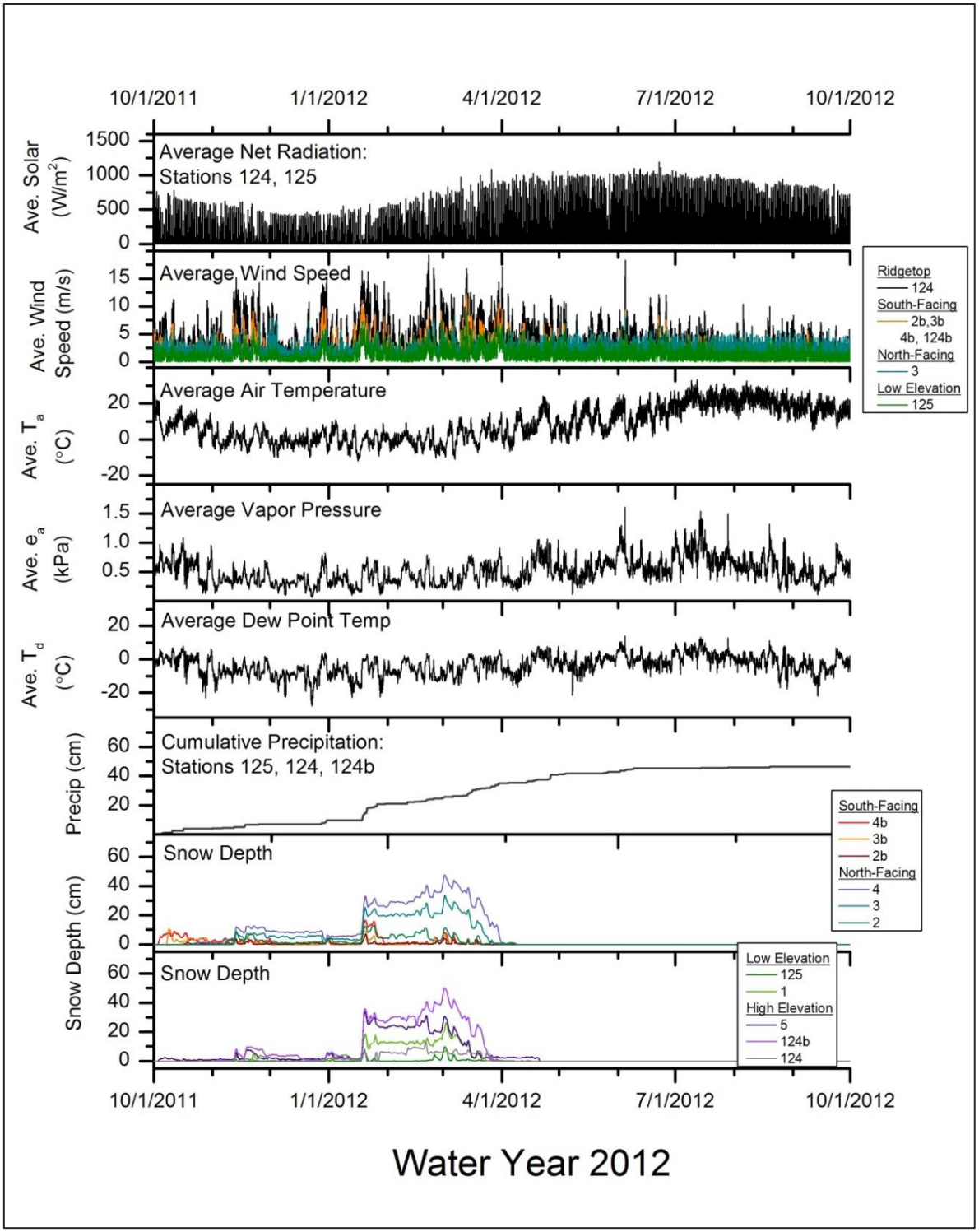

Figure B-2. Meteorological data for water year 2012 in Johnston Draw. The term "average" refers to spatial averages, rather than temporal, and includes all meteorological stations except where noted: net radiation, wind speed, and snow depth.

Appendix C. Individual event data for hydrometeorological stations in Johnston Draw

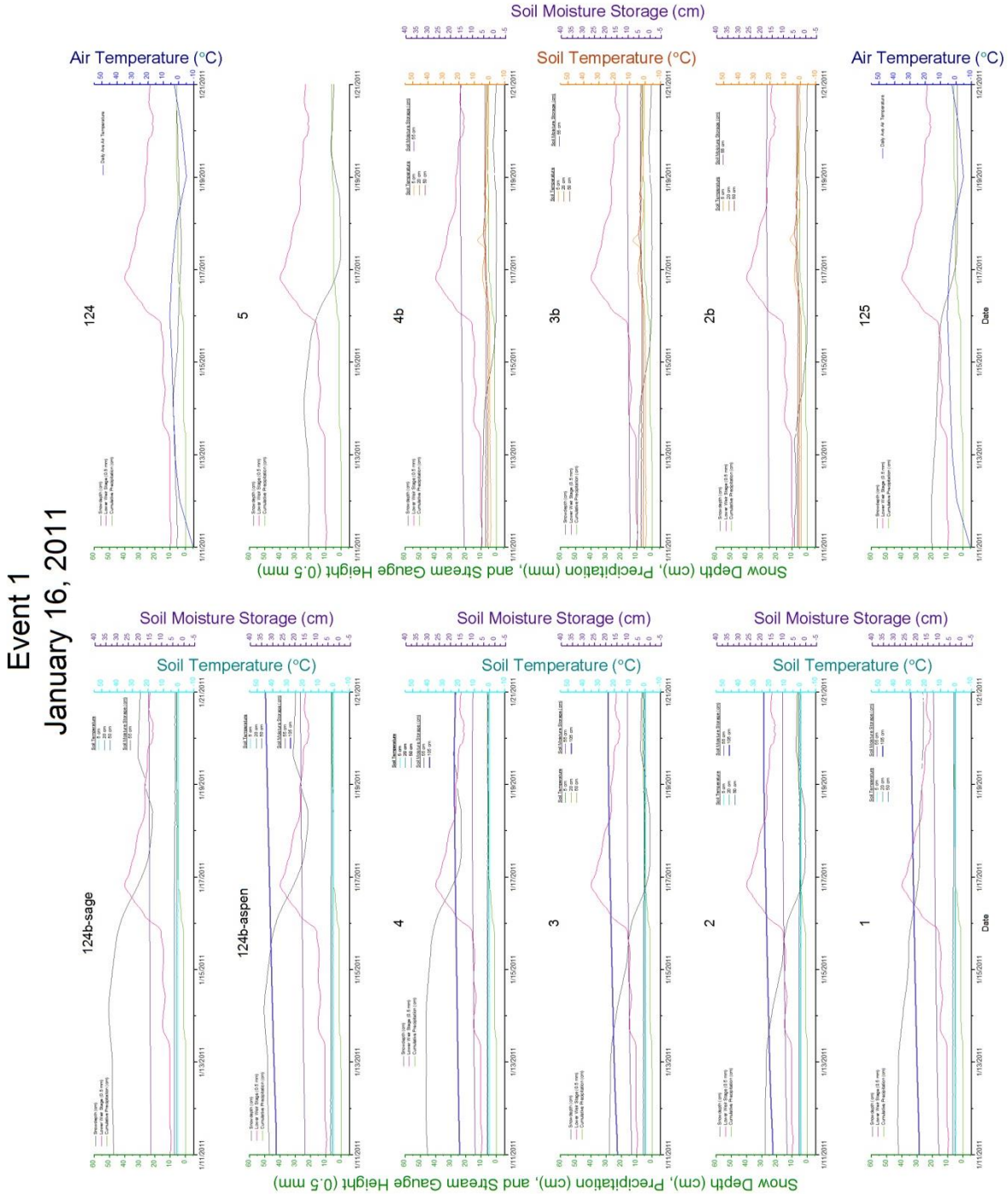

Figure C-1. Hydrometeorological data surrounding runoff generating event 1.

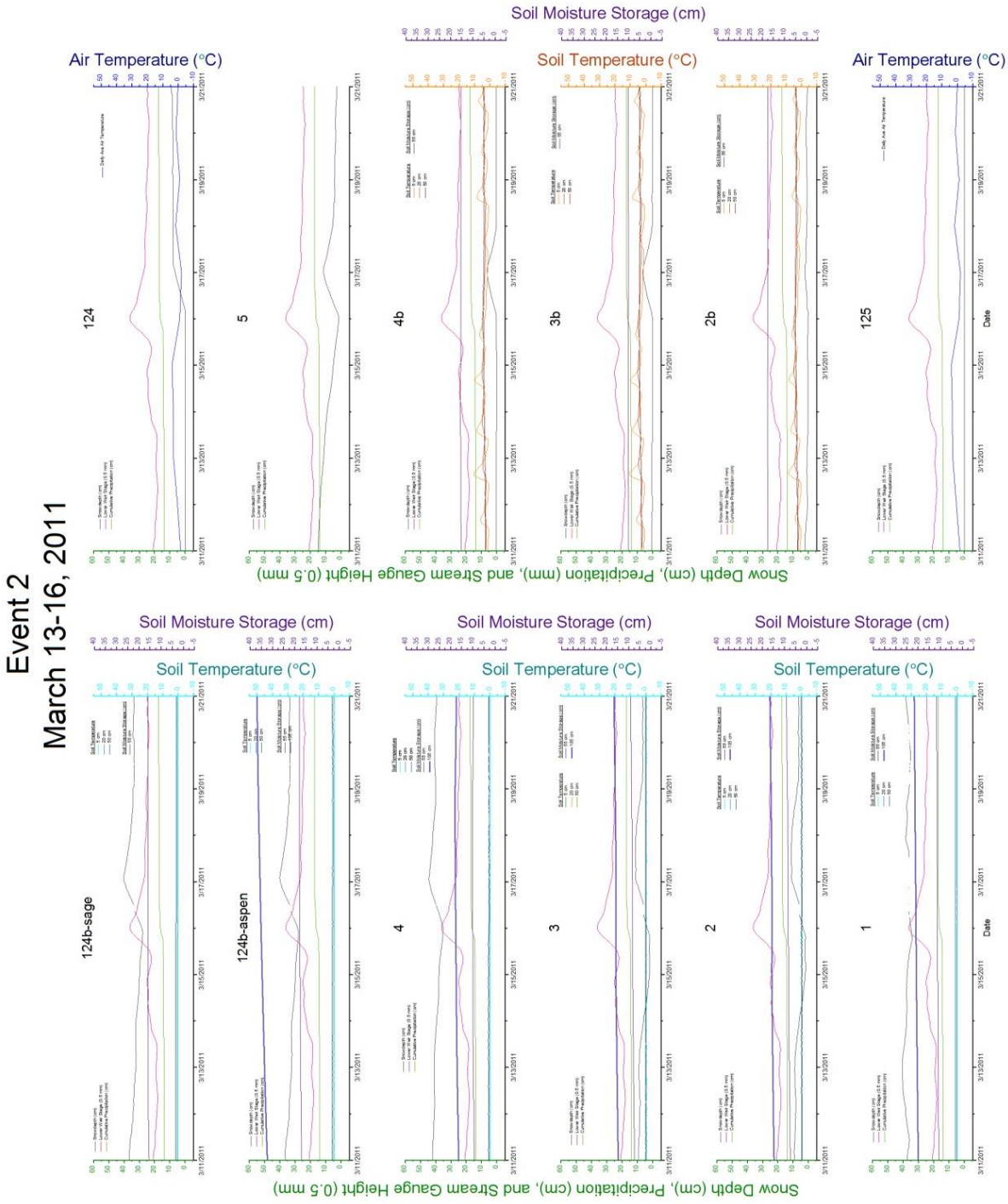

Figure C-2. Hydrometeorological data surrounding runoff generating event 2.

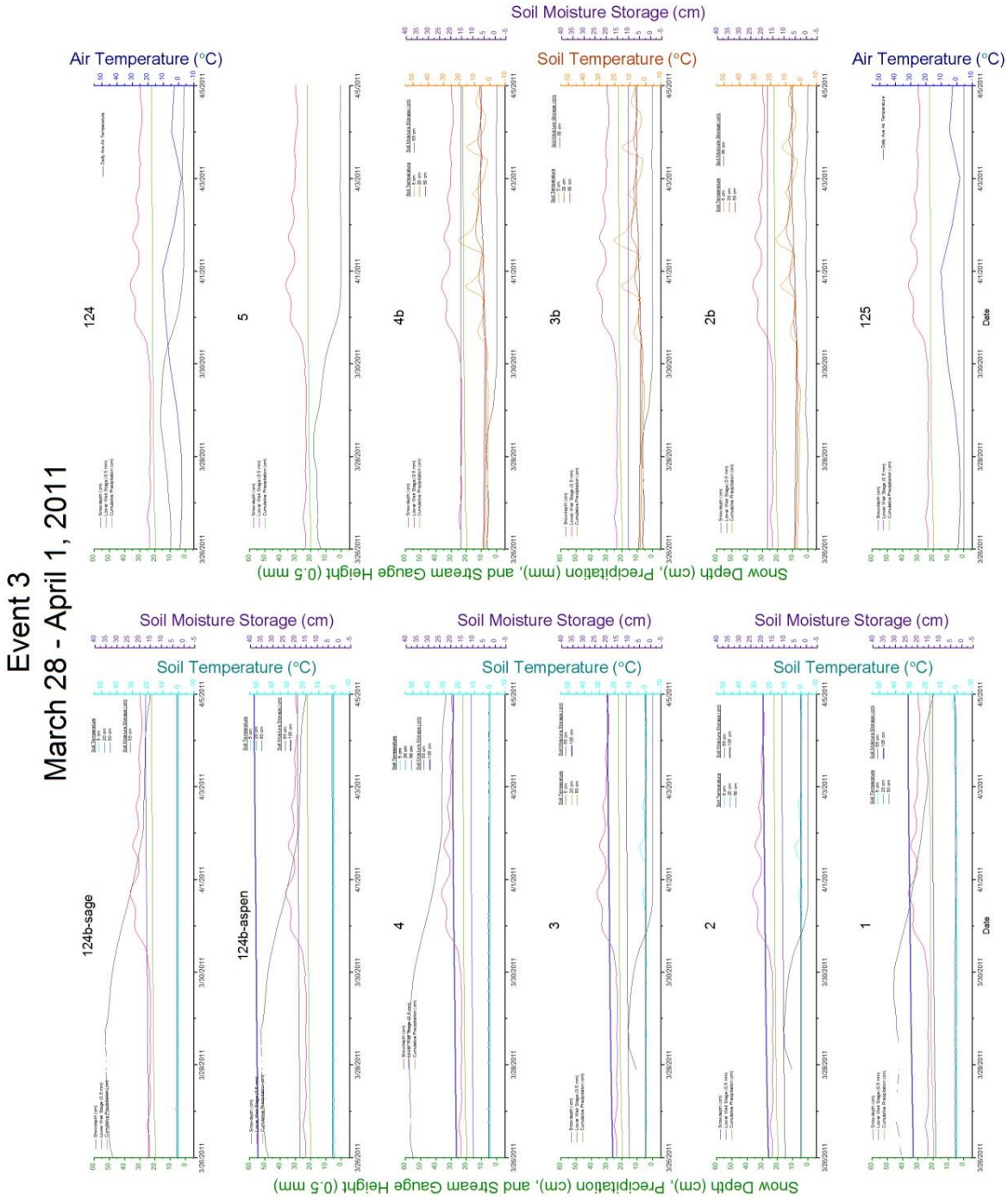

Figure C-3. Hydrometeorological data surrounding runoff generating event 3.

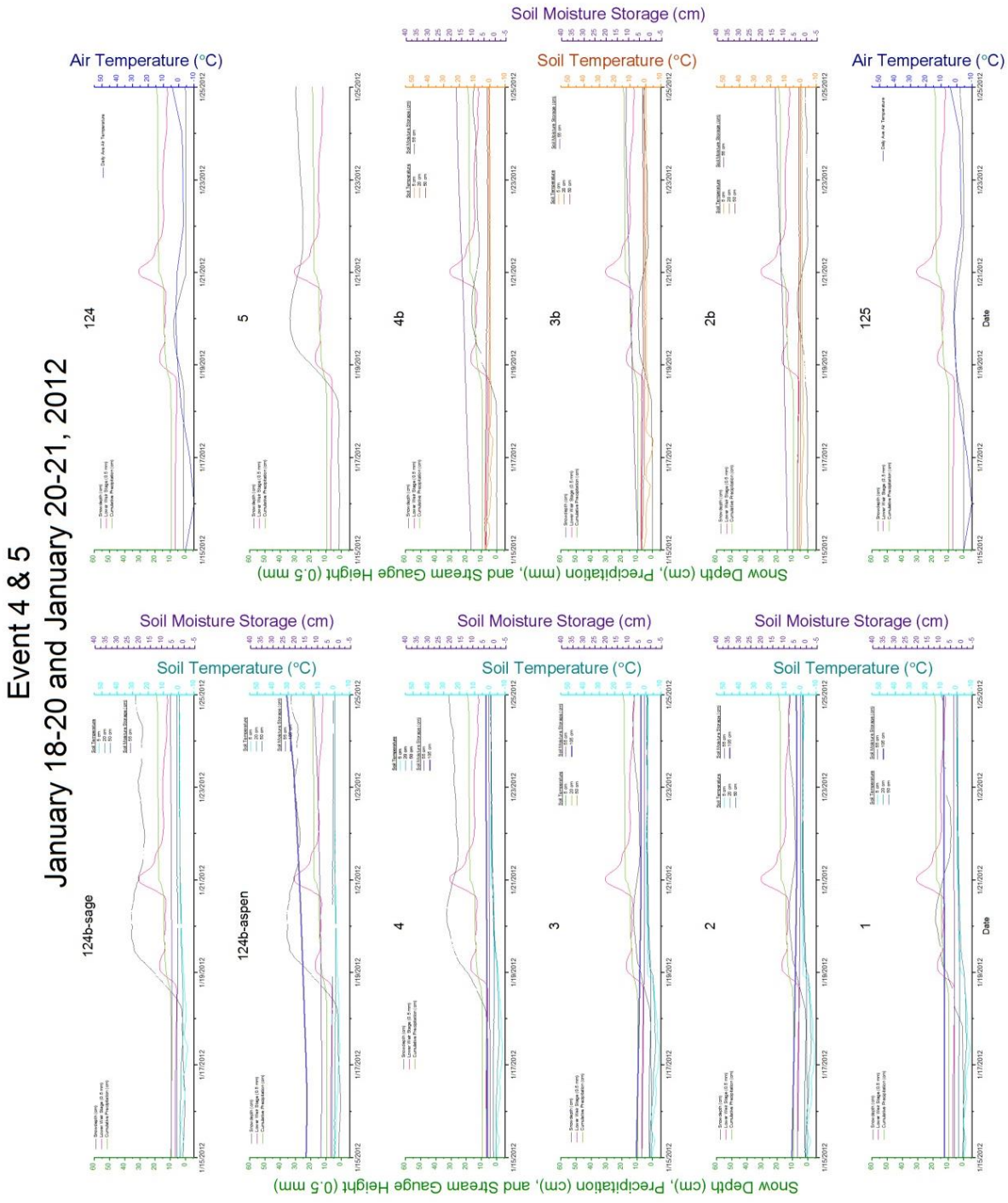

Figure C-4. Hydrometeorological data surrounding runoff generating events 4 and 5.

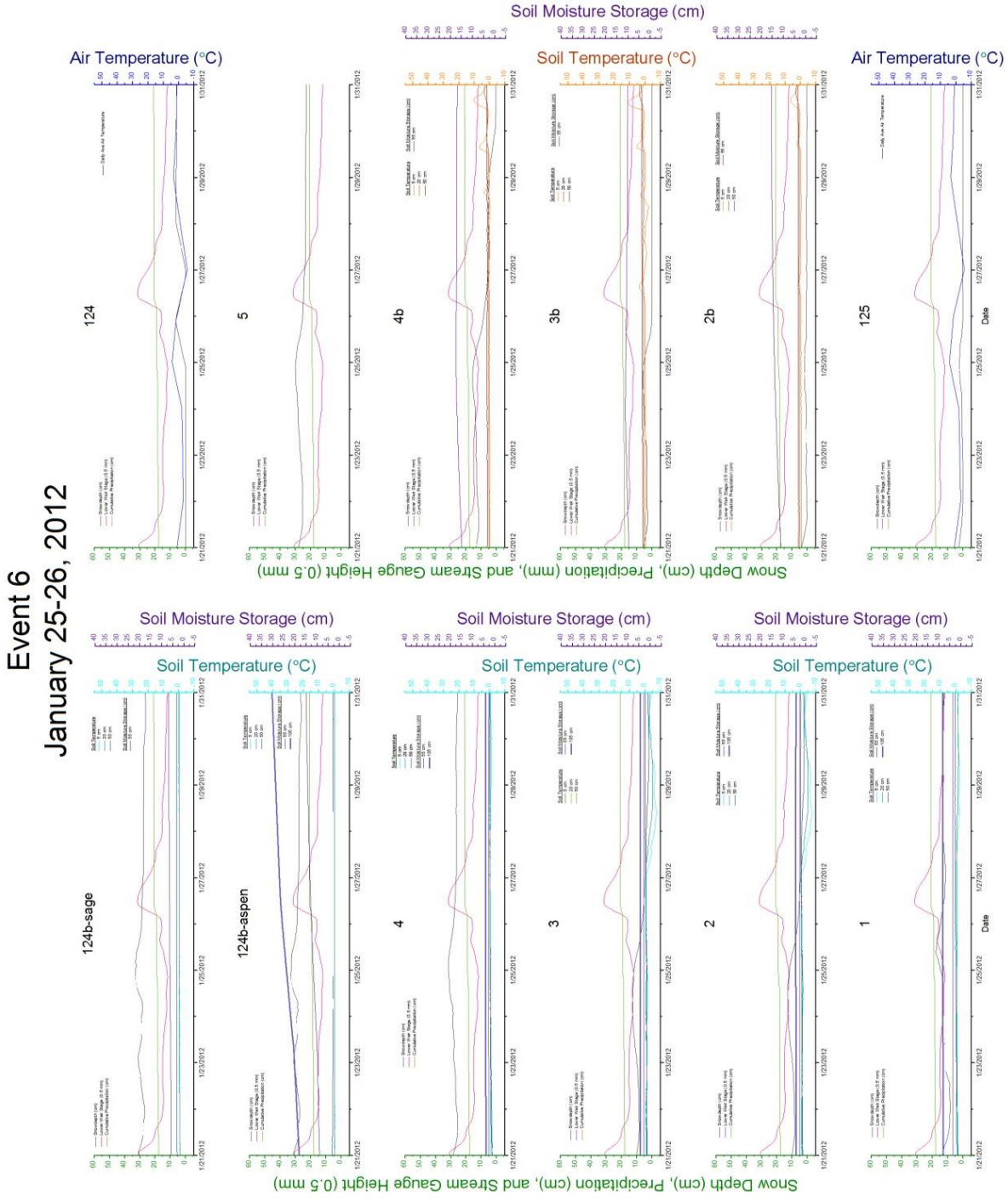

Figure C-5. Hydrometeorological data surrounding runoff generating event 6.

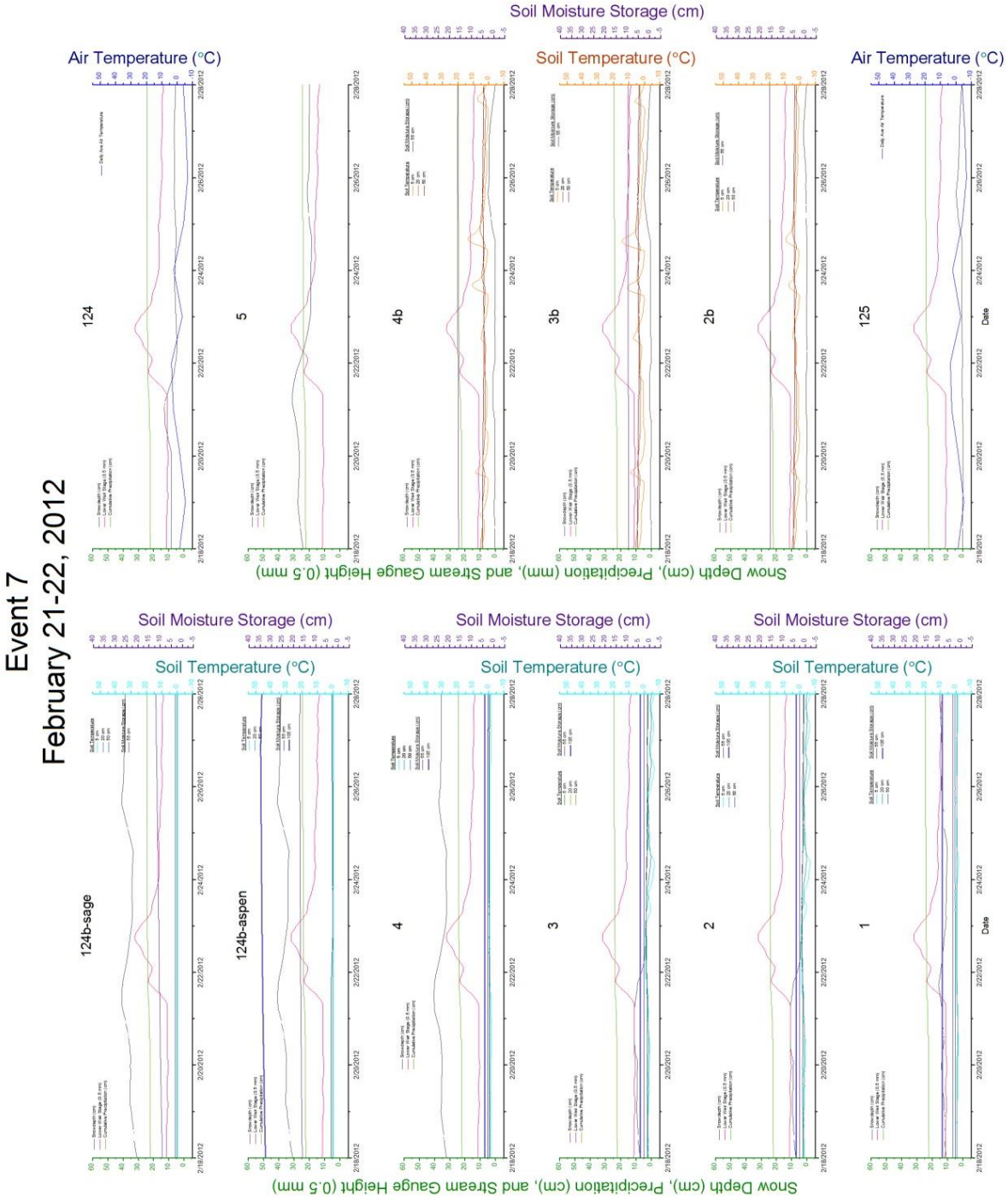

Figure C-6. Hydrometeorological data surrounding runoff generating event 7.

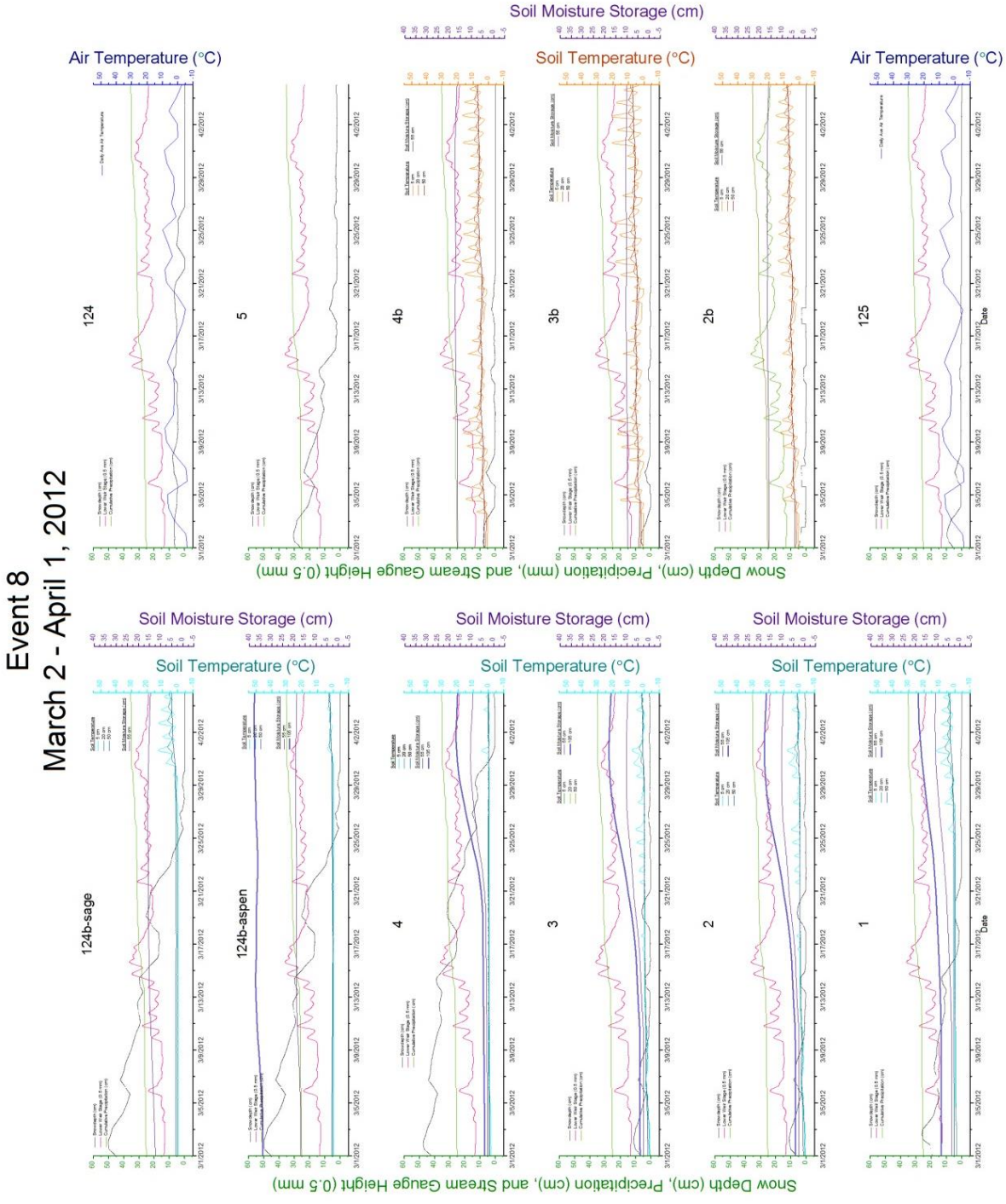

Figure C-7. Hydrometeorological data surrounding runoff generating event 8.

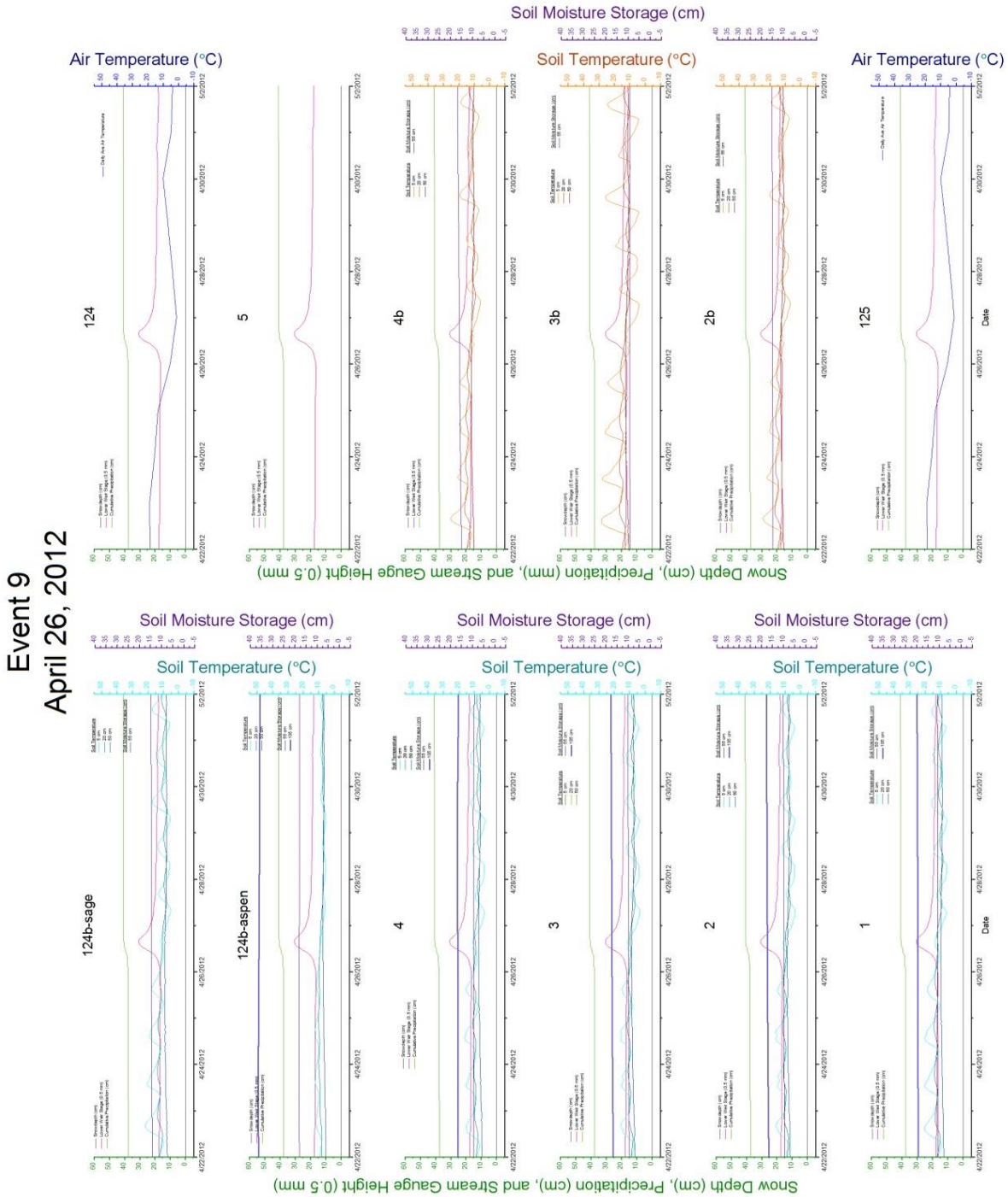

Figure C-8. Hydrometeorological data surrounding runoff generating event 9.

Table C-1. Atmospheric, surface, and subsurface conditions during runoff generation events.

			Event #	1	2.1	2.2	3	4	5	6	7	8	9	
			Event Driver	Midwinter Rain-on-snow	Early Spring Melt	Early Spring Mix Phase Precipitation	Seasonal Melt	Midwinter Mix Phase Precipitation & Melt	Midwinter Rain-on-snow	Midwinter Rain-on-snow	Midwinter melt	Seasonal Melt		Rainfall
Metric	Metric Analysis Method/Description	Metric Measurement Locations	Date	1/15/2011 20:00-1/16/2011 20:00	3/13/2011 12:00-3/15/2011 0:00	3/15/11 0:00 - 3/16/11 0:00	3/28/11 12:00-4/1/11 12:00	1/18/12 10:00-1/20/12 6:00	1/20/12 12:00-1/21/12 1:00	1/25/12 0:00-1/26/12 12:00	2/21/12 6:00-2/23/12 0:00	3/2/2012 12:00 - 4/1/12 0:00	4/26/2012
Radiation (W/m^2)	ave. of daylight hours ~730-1830, report range if multiple days	RT, LEO		47 W/m^2	267-298 W/m^2	226 W/m^2	271-514 W/m^2	43-63 W/m^2	134 W/m^2	129-182 W/m^2	123-207 W/m^2	174-466 W/m^2 (344 W/m2 ave)	232 W/m^2
Radiation % of dearsky	ave. of daylight hours ~730-1830, report range if multiple days	RT, LEO		24%	63-72%	45%	57-97%	18-32%	51%	48-68%	35-48%	39-96% (70% average)	35%
Cloud cover	estimate based on above	RT, LEO		cloudy	mostly sunny	partly cloudy	mostly sunny	cloudy	partly cloudy	partly cloudy	sunny and cloudy	mostly sunny	cloudy
T_a (°C)	all temps averaged; range of average daily	RT, HE, NFS, SFS, LE		(+) 4-6 °C	(+) 3-4°C	-1 - +4°C	0 - +10.5°C	(-)1.8-2°C	+2°C	(+)2-6°C	(+)4-7°C	-10 - +15°C (+3°C ave)	+6°C
T_d (°C)	all temps averaged; range of quarterly average	RT, HE, NFS, SFS, LE		0 - +5.5°C	(+) 1-3°C	-0.9 - +3.3°C	-9.2 - +3.7°C	-1.2 - +0.5°C	(+) 0.4-2.5°C	(+) 0.25-2°C	-4 - +4°C	-16 - +6°C (-4°C ave)	(+) 1-7°C
e_a (kPa)	all vapor pressures averaged; range of quarterly average	RT, HE, NFS, SFS, LE		0.6 - 0.9 kPa	0.4 - 0.7 kPa	0.6 - 0.8 kPa	0.3 - 0.8 kPa	0.4-0.6 kPa	0.6-0.7 kPa	0.5-0.7 kPa	0.4-0.8 kPa	0.2-0.9 kPa (0.5 ave)	0.7-0.9 kPa
Average Daily Wind Speed (m/s)	2b,3b,4b,124b averaged for SFS, range of average daily	RT, NFS, SFS		4-11 RT; 2-7 SFS; 1-3 LE, NFS	5-7 RT; 2.5-4.5 SFS; 1.8-2.4 LE, NFS	7.2 RT; 2.5-4.5 SFS; 1.5-2.7 LE, NFS	2.7-8.3 RT; 1.5-4 SFS, NFS; 1-2.2 LE	8-13 RT; 4-8 SFS; 2-4 NFS, LE	8 RT; 4.6 SFS; 2.5 NFS, LE	8-10 RT; 3-5.5 SFS, NFS; 1.5-2.7 LE	11-13 RT; 5 SFS; 3-4 NFS; 2-3 LE	1-9 RT (6 ave); 1-6 SFS, NFS, LE (3 ave)	6 RT; 2-3 NFS, SFS, LE
Precip (cm)	difference over time period	RT, LEO		3.5	0	2.1	0.4	4.7	3.2	1.6	1	9.6	2.8
Precipitation Phase	based on air temp, dew point temp, and changes in snowpack (if present)	RT, HE, NFS, SFS, LE		rain	na	rain transition to snow	rain	snow, transition to snow mixed with rain, transition to snow	rain	rain	rain	rain and snow	rain
Δ Snow depth (cm)	change over time period	RT, HE, NFS, SFS, LE		-24-28 HE, NFS; -11-13 LE; -7-8 SFS (ablated); -5 RT	-5-10 HE; -5-7 NFS; -0.4 SFS, LE(ablated)	-2.4-2.8 NFS (Ø sta 2), -1.9-3.5 HE; Ø LE, RT, SFS	-15 -24 RT, HE, NFS, LEN (RT, HE 5, NFS 2 ablated); -1-7 SFS (ablated); Ø LEO	+33 HE; +11-26 NFS, LEN; +7-16 SFS; +6-8 RT, LEO	-3.8-4.5 RT(ablated), HE, LEN; -2.3-3.9 NFS, SFS, LEO	-5-8 RT, HE, NFS, SFS (sta 2b, 3b ablated), LEN; -2 LEO (ablated)	-6-12 RT, HE, NFS; -3 LEN; -1-2 SFS (ablated); (na) LEO	Complete ablation: -11-50 HE, NFS; -8-10 RT, LEO; -5-8 SFS	na
Δ Soil Temp at 20 cm depth (°C)	change over time period	HE aspen, HE sage, NFS, SFS, LEN		+1.8 SFS; Ø RT, HE, NFS, LEN	+ 0.5-1 SFS; Ø RT, HE, NFS, LEN	-0.6 SFS; Ø RT, HE, NFS, LEN	+4.4 SFS; Ø RT, HE, NFS, LEN	+4-5 NFS, LEN; +1-2 HE sage; Ø SFS, HE aspen	+0.3-0.5 RT, HE, NFS, LEN; Ø SFS	Ø	+0.5-0.8 SFS; Ø HE, NFS, LEN	+5-6 SFS, HE sage, LEN; +1-4 NFS, HE aspen	-1.3-1.5°C SFS, HE sage: -0.3-0.9°C NFS, HE aspen
Δ Soil Temp Diurnal Flux at 20 cm (°C)	change over time period	HE aspen, HE sage, NFS, SFS, LEN		+1.9-2.2 SFS; Ø RT, HE, NFS, LEN	- 0.5-1 SFS; Ø HE, NFS, LEN	+0.6 SFS; Ø HE, NFS, LEN	+4.2 SFS; Ø RT, HE, NFS, LE	+0.6-1.9 NFS, LEN; 0.4 HE sage; Ø SFS, HE aspen	Ø	Ø	+0.3-0.7 SFS; -0.6 NFS (sta 2); Ø NFS, HE, LEN	+2-3 HE, NFS, LEN; Ø SFS	Ø
Frozen Soil	Locations where frozen; soil moisture unknown	1,2,3,4,124ba, 124bs,2b,3b, 4b		2			2,3	124bs, 1,2,3,4	124bs, 1,2,3,4	124bs, 1,2,3,4	2,3,4	1,2,3,4	
Δ 55 cm Soil Moisture Storage (cm)	change over time period	HE aspen, HE sage, NFS, SFS, LEN		+0.3-0.5 HE, NFS, SFS, LEN	+0.2-0.4 NFS,LEN; +0.1-0.3 HE; Ø SFS	+0-0.1 NFS, HE, LEN; Ø SFS	+0.4-0.7 NFS, HE, LEN; Ø SFS	+0.8-1.1 SFS; +0.4 HE aspen; (u) HE sage, NFS, LEN	+0.4-0.5 SFS; +0.2 HE aspen; (u) HE sage, NFS, LEN	+1.3 HE aspen; Ø SFS, (u) HE sage, NFS, LEN	Ø	+2.1-2.6 HE; +0.6-0.9 SFS; (u) NSF, LEN	Ø
Δ 105 cm Soil Moisture Storage (cm)	change over time period	HE aspen, NFS, LEN		+ 0.6-0.9 HE aspen, NFS, LEN	+0.4-0.5 NFS,LEN; +1.1 HE aspen	+0-0.2 NFS; HE aspen, LEN	+0.6-1.1 NFS, HE aspen, LEN	+1.4 HE aspen; (u) NFS, LEN	+0.6 HE aspen; (u) NFS, LEN	+2.6 HE aspen; (u) NFS, LEN	+0.4 HE aspen; (u) NFS, LEN	+3.8 HE aspen; (u) NFS, LEN	Ø
Δ Weir Stage (cm)	change over time period			+ 4.8	+1.1	+2.8	+2.7	+2.2	+3.6	+3.8	+4.2	+2 - 4	+2.8

Abbreviations:
(na)= not applicable; (u)= unknown; Ø= no significant change
RT= ridgetop (124); HE= high elevation (124b, 5); HE aspen= high elevation aspen canopy (124ba); HE sage= high elevation sage (124bs); NFS= north facing slope (2, 3, 4); SFS= south facing slope (2b, 3b, 4b); LE= low elevation (125, 1); LEN= low elevation north (1); LEO= low elevation outlet (125)